菱刈鉱山地域火山岩の古地球磁場強度と磁気特性

著者	上野 直子，鄭 重，上野 宏共
雑誌名	東洋大学紀要．自然科学篇
号	56
ページ	141-175
発行年	2012-03
URL	http://id.nii.ac.jp/1060/00005329/

Paleointensity and Rockmagnetism of the Hishikari Mining Area, Kyushu, Japan

Naoko UENO*, Zhong ZHENG** and Hirotomo UENO***

Abstract

Pleistcene igneous rocks dated by K-Ar and fission-track methods were used to extract the paleomagnetic intensity of the geomagnetic field. Rockmagnetic characters of hysteresis curve, hysteresis parameters, Curie temperature and susceptibility change with temperature were measured to find the correlation with the result of paleointensity. Thelliers' method could not derive any long straight line in Arai diagram. Moreover, Zheng's method succeeded only in one sample. The main reasons of the failure were thermo-chemical alteration and unstable remanent magnetic property of rocks during the laboratory heating process. For most of the samples, the blocking temperature spectra have shifted toward the lower temperature side after heating. A good result by Zheng's method, which being conducted successfully the correction of grains magneto-static interaction, from Shishimano dacite yields 46+/−3 μT.

Keywords: Hishikari, Paleointensity, Pleistcene, Thelliers' method, Zheng's method

1. Introduction

The Hishikari mine (32° 05'N. 130° 41'E) is located in Kagoshima Prefecture, Kyushu, Japan (Fig.1.). The geological sequences in the area are divided in two main groups: the Shimanto Supergroupe of Cretaceous and volcanic rocks of Pleistocene.

The Pleistcene volcanic rocks composed of andesite and dacite are divided into five

*) 上野直子：東洋大学自然科学研究室　〒 112-8606　東京都文京区白山 5-28-20
Natural Science Laboratory, Toyo University, 5-28-20, Hakusan, Bunkyouku, Tokyo 112-8606, JAPAN: ueno@toyo.jp
**) 鄭　重：綜合開発株式会社地球科学事業部　〒 133-0057　東京都江戸川区西小岩 1-30-16 三幸ビル 2 号館
Sogo Kaihatu Co., Sanko Build., 1-30-16, Nishikoiwa, Edogawaku, Tokyo 133-0057, JAPAN: tei-cho@sogo-geo.co.jp
***) 上野宏共：千葉科学大学環境安全システム学科　〒 288-0025　千葉県銚子市潮見町 3
現住所：〒 989-3123　仙台市青葉区錦ケ丘 6-20-8
Department of Enviromental Security Systems, Chiba Institute of Science, 3 Shiomicho, Choshishi 288-0025, JAPAN.
Present address: 6-20-8 Nisikigaoka, Aobaku, Sendaishi 989-3123, JAPAN.

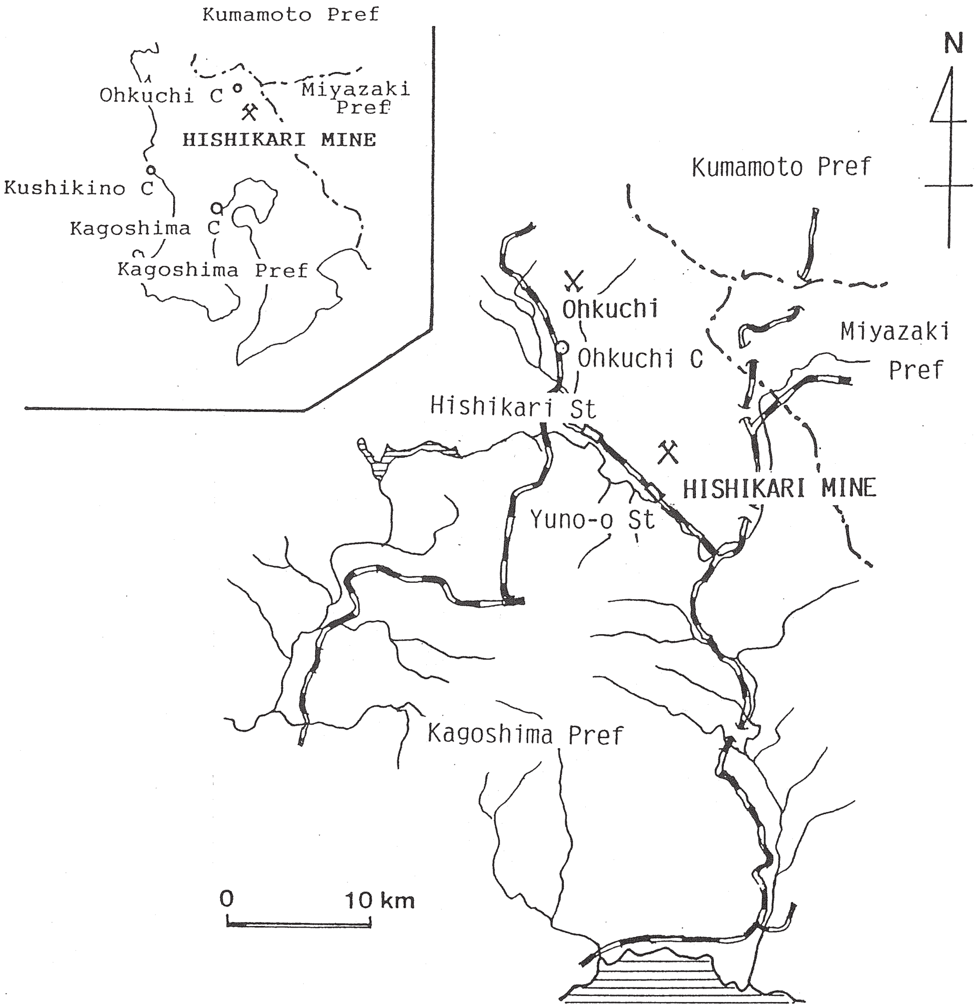

Fig. 1 Location map of the Hishikari mining area. (original map: Ueno et al 1987)

formations as shown in Fig.2. In this area, about one hundred data of absolute ages of Pleistcene volcanic rocks by K-Ar and fission track methods are accumulated (Metal Mining Agency of Japan and Sumitomo Metal Mining Co., Ltd., 1987). The geomagnetic polarity sequences were also studied and described in detail by Ueno et al.(1987) and Ueno (2007) as shown in Fig. 2. Combining (i) geological sequences, (ii) absolute ages, and (iii) magnetic polality , it is suggested that the volcanic rocks were erupted during the 5 changes of polarity in Pleistocene.

The aim of this study was to reveal the magnetic property of constituting igneous rocks, and to estimate the intensity variation of geomagnetic field during the polarity changes.

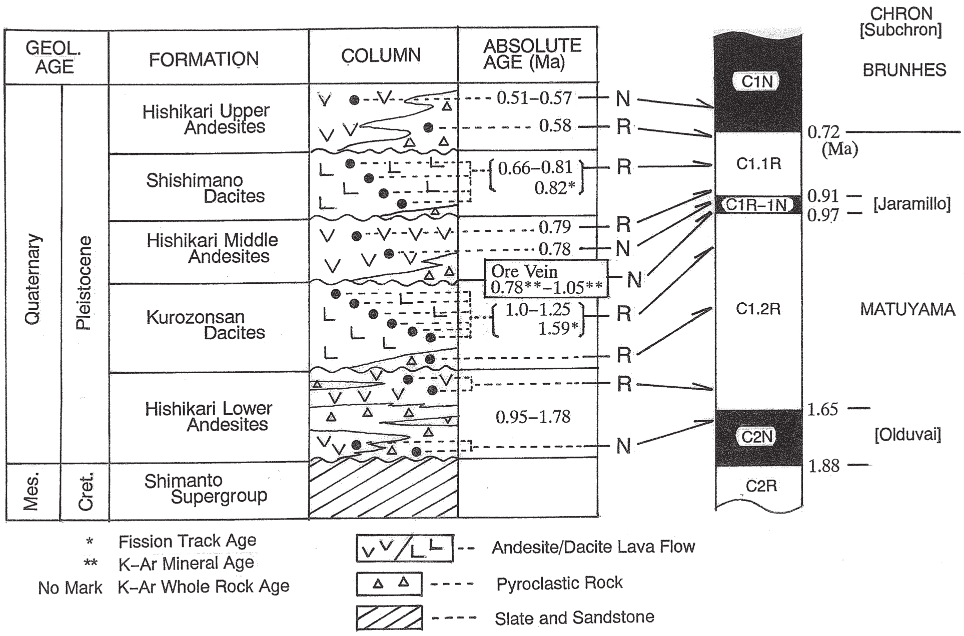

Fig. 2 Geological column and magnetic sequence in the Hishikari mining area.

2. Samples

Sampling was carried near the age dating point as shown in Fig.3. The sampling points were plotted also on the geological map Fig.4 . Some representative outcrop photos are presented in Fig.5. Sample number with formation and magnetic sequence was listed in Table 1.

3. VSM Characters of Rockmagnetism

To understand the general character of the rockmagnetism, VSM (Vibrating Sample Magnetometer) was used to draw hysteresis loops, Js-T (saturated magnetization variation with temperature change) curves and Day diagram. Fig.6 shows some examples of hysteresis loops. Hc (coercivity) varies from 80 Oe to 200 Oe, and Table 2 summarizes the main parameters of the result of VSM experiment.

Some representative examples of Js-T curves are showed in Fig,7-1 and 7-2. The general feature of irreversible curves strongly suggests somewhat mineral change occurred in heating process. VSM made by Riken Denshi Co. was used at the magnetic field of 10kG, in vacuum of 10^{-5} Torr. Day diagram illustrated in Fig.8 indicates the main magnetic minerals are dotted in pseudo-single domain region of titano-magnetites.

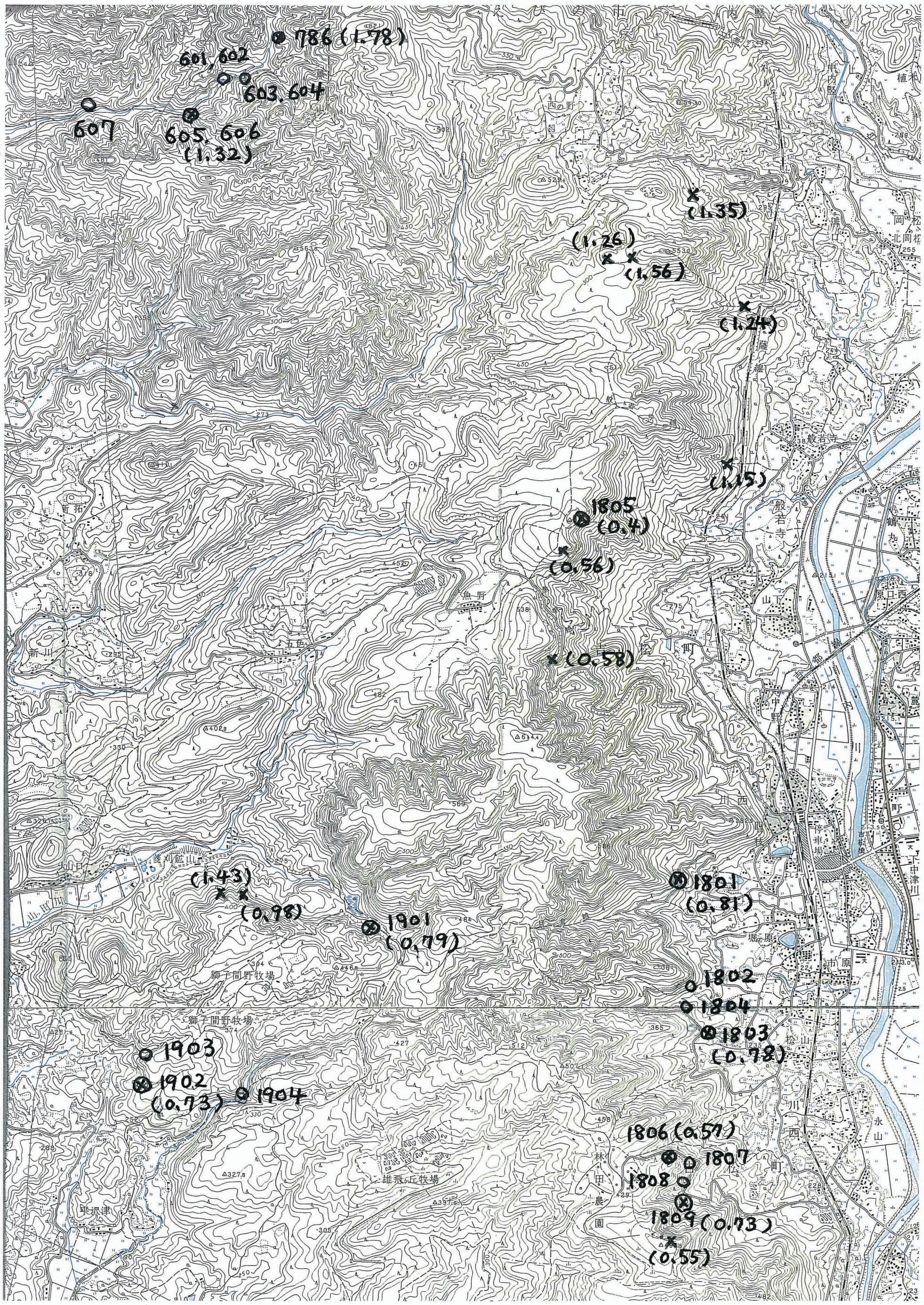

Fig.3 Sampling site (original map: 国土地理院地形図 栗野)
○ sampling point
× dating point (Ma)

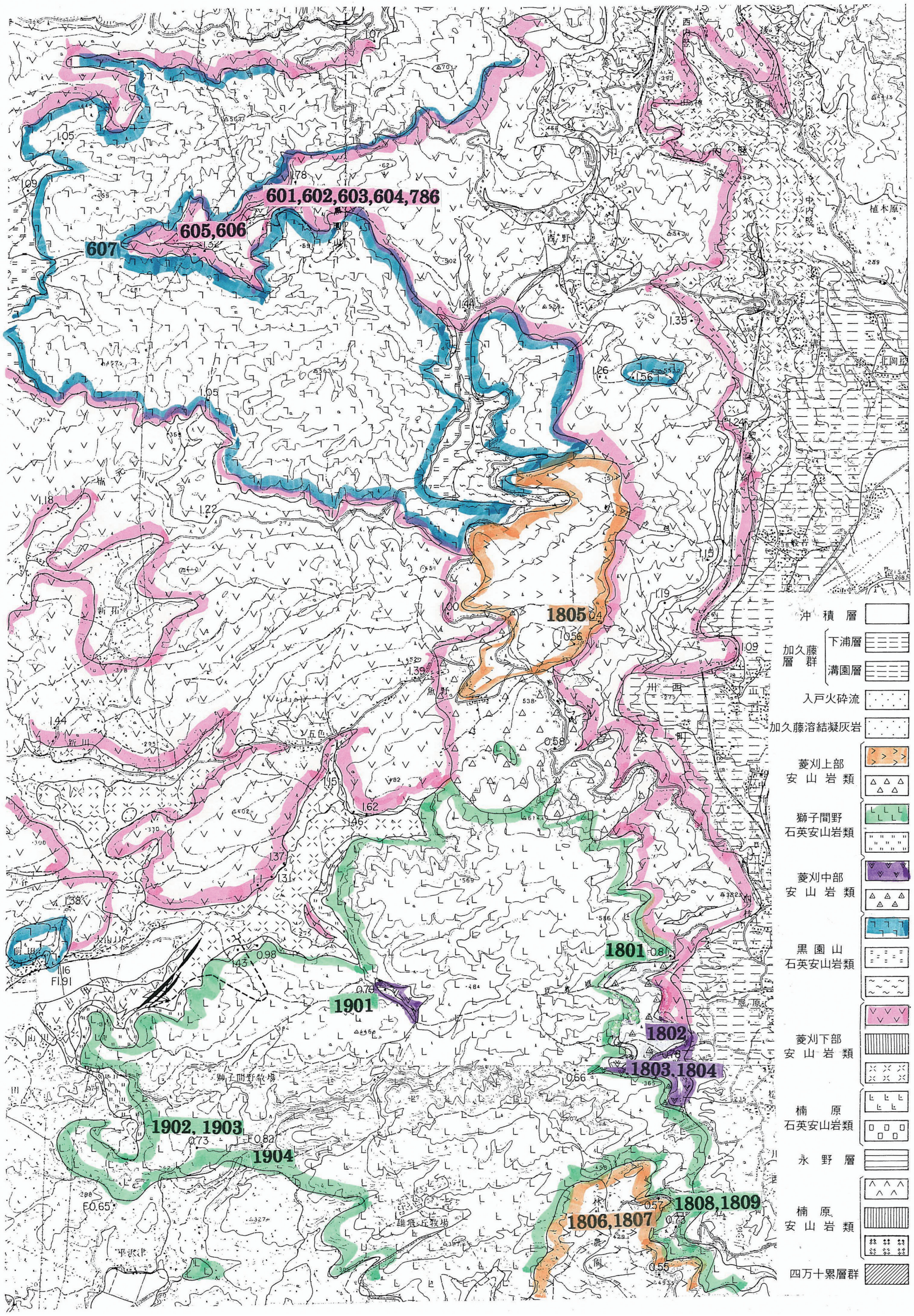

Fig.4 Geological map with absolute age dating point (Ma) of sampling site. (original map: 住友金属鉱山株式会社作成地質図 栗野, 吉松)

Fig.5 Pictures of the sampling site
the upper left ---1801 the upper right ---1803 (this side), 1804 (far side)
the lower left ---1802 the lower right ---1903

Table 1. Sample number and formation/ magnetic sequence

Formation	Sample No.	Magnetic Sequence
Hishikari Upper Andesites 菱刈上部	1805, 1806, 1807	BRUNHES (N)
ShishimanoDacites 獅子間野	1801, 1808, 1809 1901, 1902, 1903 1904	MATSUYA MA (R)
Hishikari Middle Andesites 菱刈中部	1802, 1803, 1804	JARAMILLO (N)
Kurozonsan Dacites 黒園山	607	MATSUYAMA (R)
Hishikari Lower Andesites 菱刈下部	605, 606	MATSUYAMA (R)
	601, 602, 603 604, 786	OLDUVAI (N)

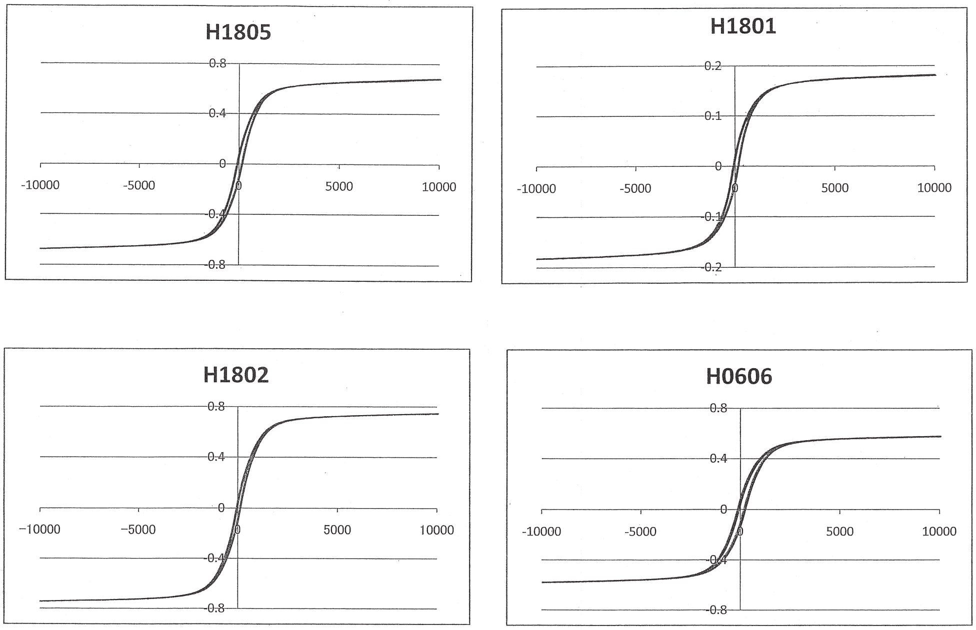

Fig.6 Examples of hysteresis curve

Table 2. Results of VSM experiments

Formation	Sample No.	Sample weight for VSM (mg)	$Msx10^{-1}$emu	$Mrsx10^{-2}$ emu	Hc oe	Hcr oe	Mrs/Ms	Hcr/Hc	Tc °C
Hishikari Upper Andesites (N)	1805	511.7	6.77	8.65	119	186	0.128	1.56	–
	1806	280.3	5.26	5.79	144	288	0.110	2.00	520
	1807	574.1	8.35	9.78	114	253	0.117	2.22	–
Shishimano Dacites (R)	1801	361.0	1.82	2.44	113	200	0.134	1.77	515
	1808	331.4	1.26	2.09	141	279	0.166	1.99	420, 540
	1809	401.5	1.74	3.12	164	284	0.179	1.73	–
	1901	380.9	5.93	7.59	126	226	0.128	1.79	–
	1902	349.7	1.71	2.67	128	150	0.156	1.17	–
	1903	324.5	1.58	2.36	122	224	0.184	1.84	–
	1904	364.3	2.14	3.60	195	373	0.168	1.91	540
Hishikari Middle Andesites (N)	1802	397.5	7.45	6.86	87	141	0.092	1.62	–
	1803	415.3	5.29	8.52	152	279	0.161	1.84	–
	1804	317.0	3.95	3.58	81	146	0.091	1.80	450, 555
Kurozonsan Dacites (R)	607	380.0	2.70	3.75	143	216	0.149	1.51	512
Hishikari Lower Andesites (R)	605	334.3	4.61	5.50	107	185	0.119	1.73	525
	606	442.1	5.76	9.01	159	292	0.156	1.84	–
(N)	601	493.2	6.58	6.00	81	134	0.091	1.65	–
	602	461.8	6.02	5.87	88	153	0.098	1.74	–
	603	604.2	6.55	10.10	164	310	0.154	1.89	–
	604	253.8	3.12	4.59	158	314	0.147	1.99	350, 548
	786	334.0	3.36	4.06	103	180	0.121	1.75	245, 509

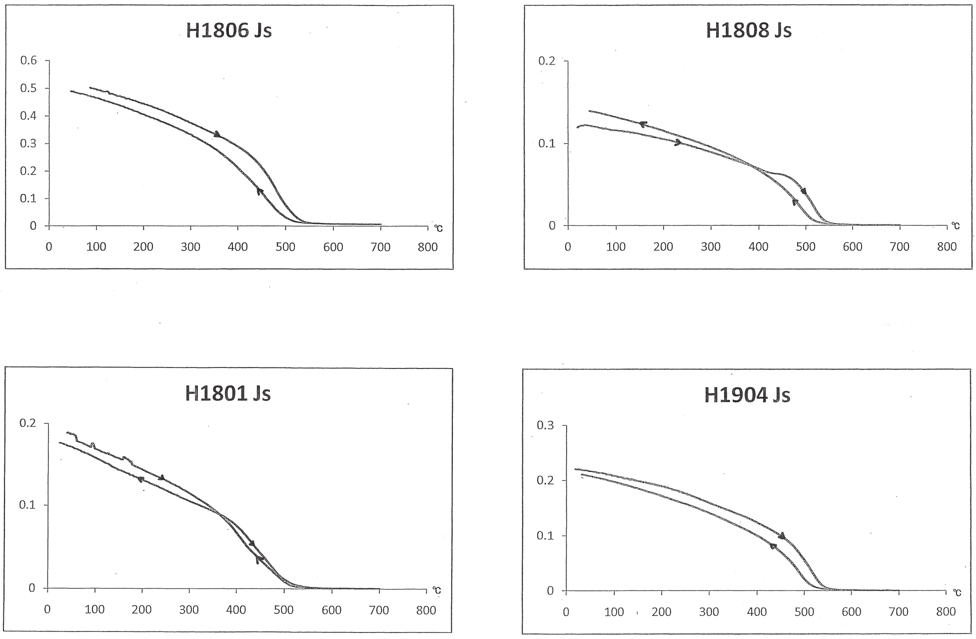

Fig.7-1 Examples of Js-T curves

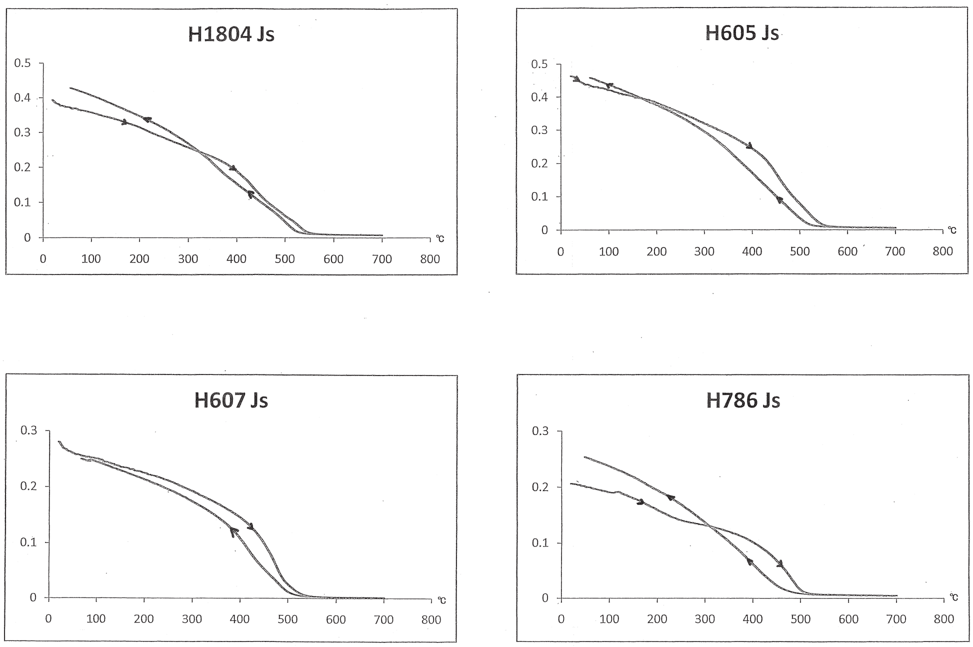

Fig.7-2 Examples of Js-T curves

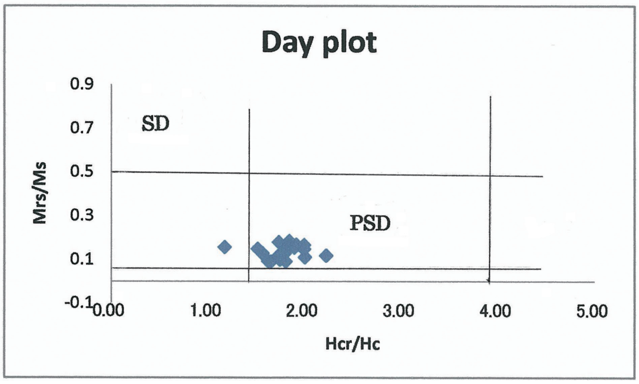

Fig.8 Day Diagram

4. Paleointensity by Thelliers' Method

The Coe's version of the Thelliers' method was carried in the laboratory of Tokyo Institute of Technology a long time ago. Some Arai diagrams of those results were illustrated in Fig.9-1~Fig.9-8. Procedures and conditions are as follows: specimens are 25mm in diameter,10mm to 22mm in length: treated in a series of paired heating-cooling cycles, repeated in zero and known laboratory field with progressively increasing temperature: nitrogen atmosphere above 100℃: pTRM test was employed for every sample.

All the specimens failed to yield long straight lines in Arai diagram. For the reason, it can not expect to calculate a constant intensity of ancient geomagnetic field (H_{an}). The reasons of off-lines in Arai diagram were considered to be both chemical alteration during heating and magneto-static interaction effect of magnetic grains as suggested in detail in next section 5.

Fig.10. shows χ-T (the variation of initial susceptibility with temperature change) during the Thelliers' experiment measured by Bartington instruments.

5. Paleointensity by Zheng's Method

Zheng's method for paleointensity determination was introduced in the several previous reports (Ueno et al. 2005; Ueno et al. 2008; Ueno and Zheng 2010; Ueno and Zheng 2011; Ueno and Zheng 2012; Zheng et al.2005; Zheng and Zhao 2006). The experiments of Zheng's method were carried in a furnace made by Sogo Kaihatsu Co, under vacuum atmosphere about 0.1 Pa.

Briefly, the Zheng's method requires the following condition:

(Continued on page 154)

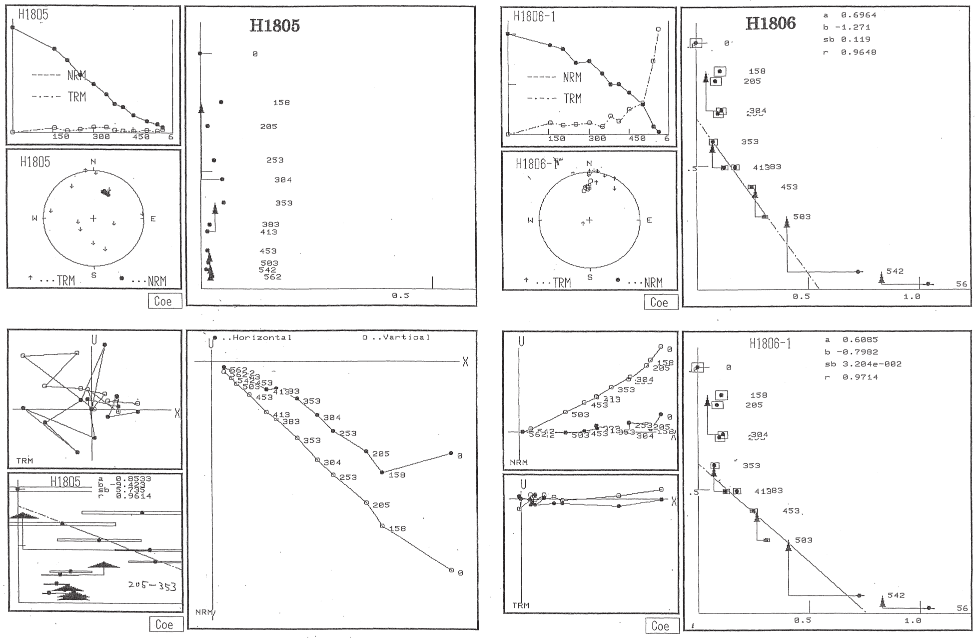

Fig.9-1 Arai Diagram of the Hishikari Upper (N) : Laboratory Field H_0=40μT

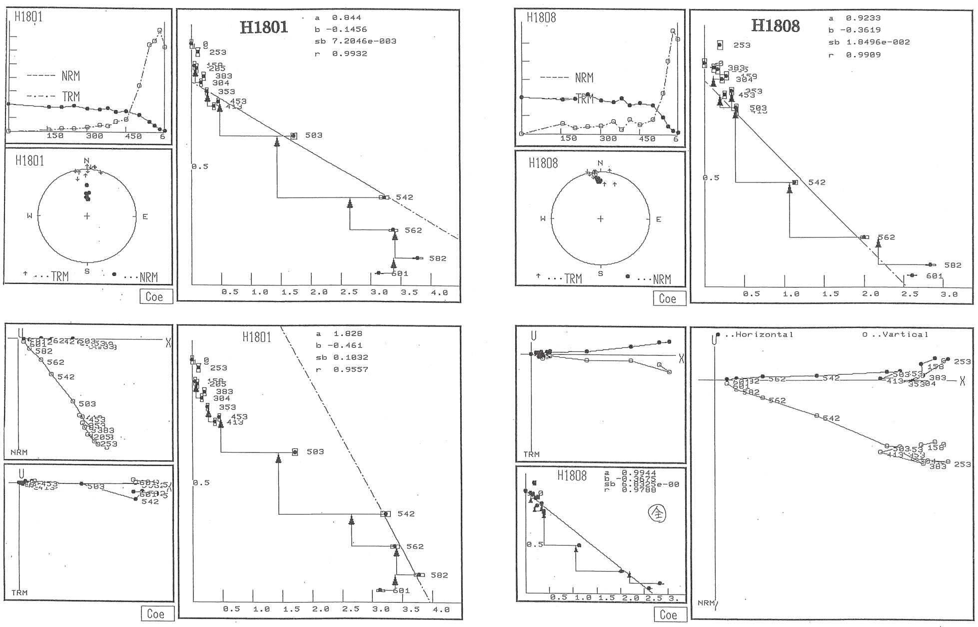

Fig.9-2 Arai Diagram of the Shishimano (R) : H_0=40μT

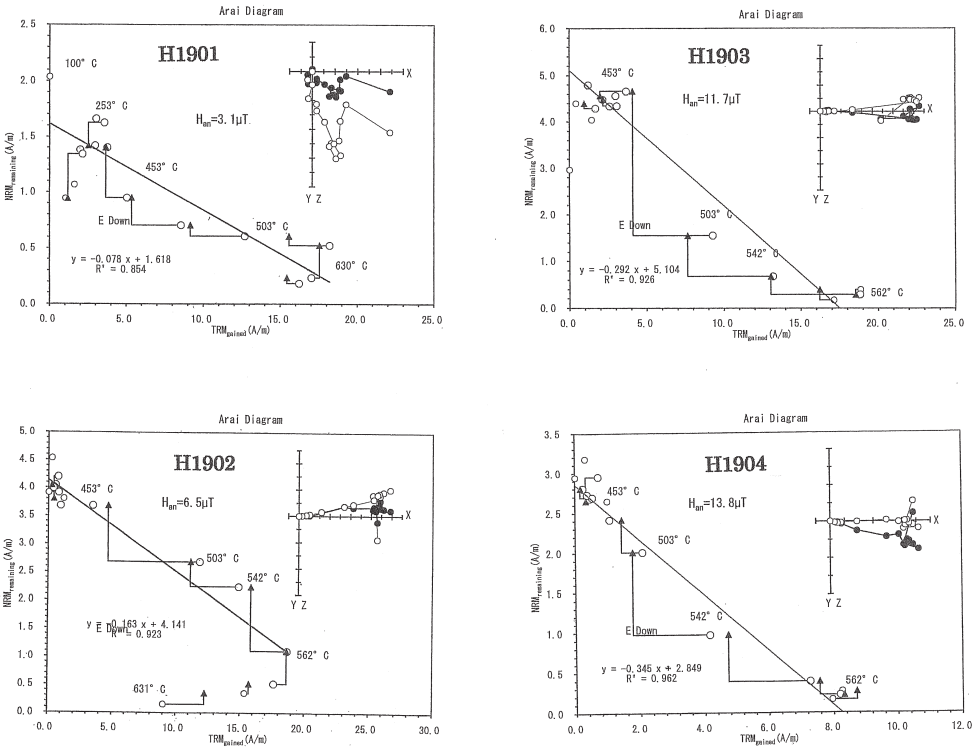

Fig.9-3 Arai Diagram of the Shishimano (R) : H_0=40μT

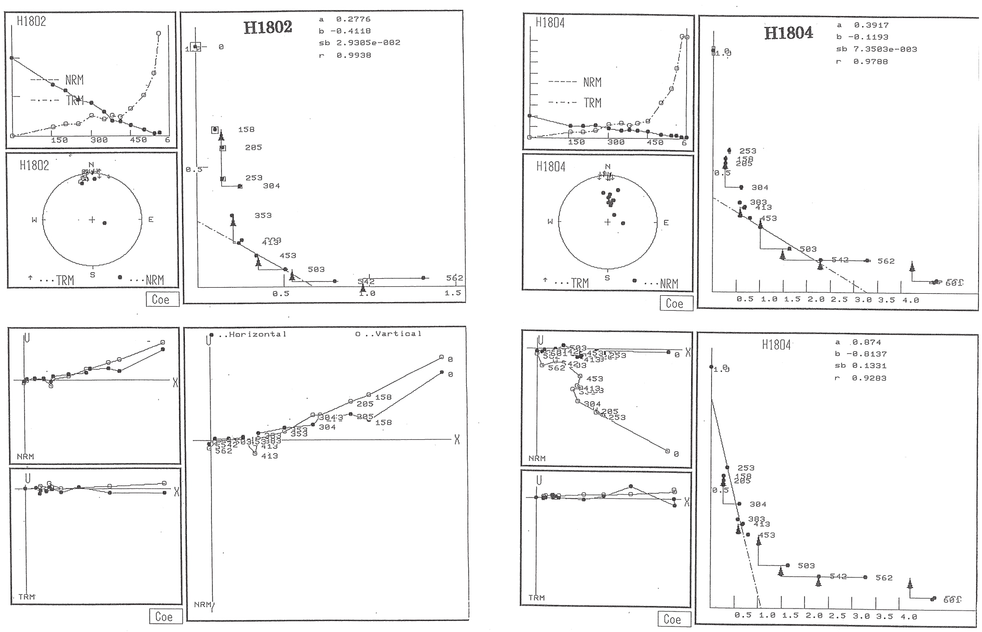

Fig.9-4 Arai Diagram of the Hishikari Middle (N) : H0=40μT

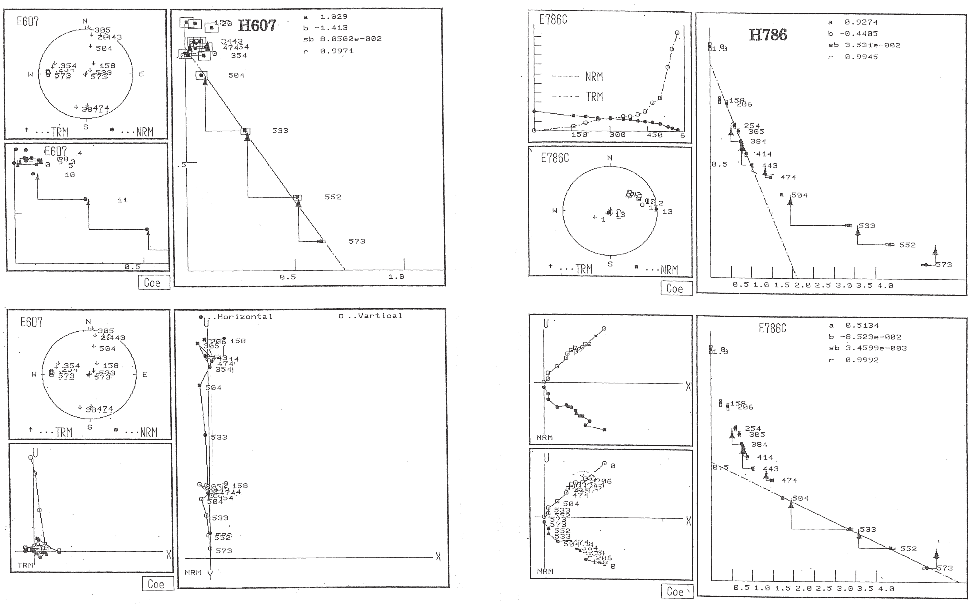

Fig.9-5 Arai Diagram of the Kurozonsan (R) and the Hishikari Lower (N) : H_0=50μT

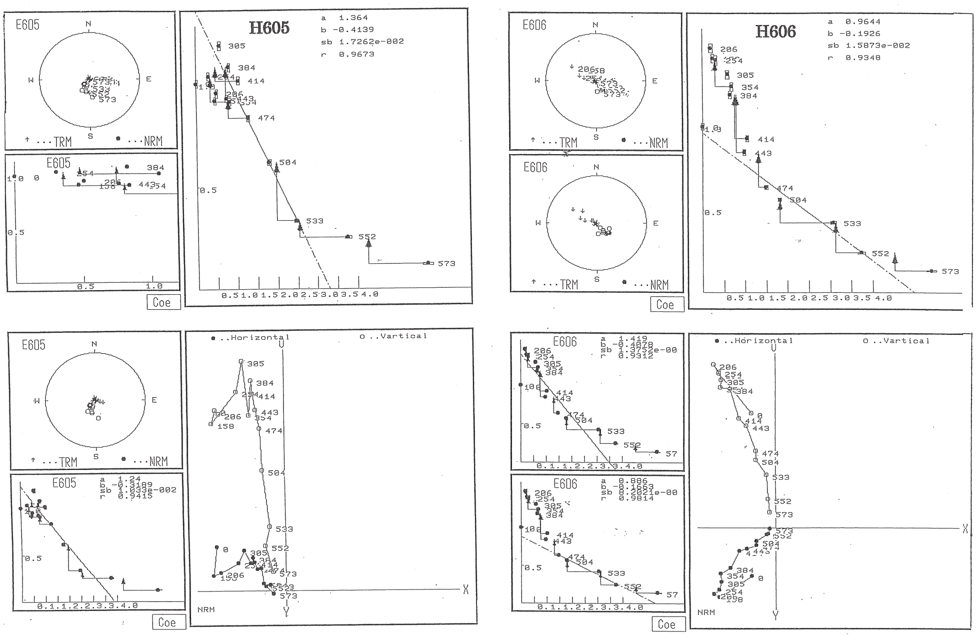

Fig.9-6 Arai Diagram of the Hishikari Lower (R): H_0=50μT

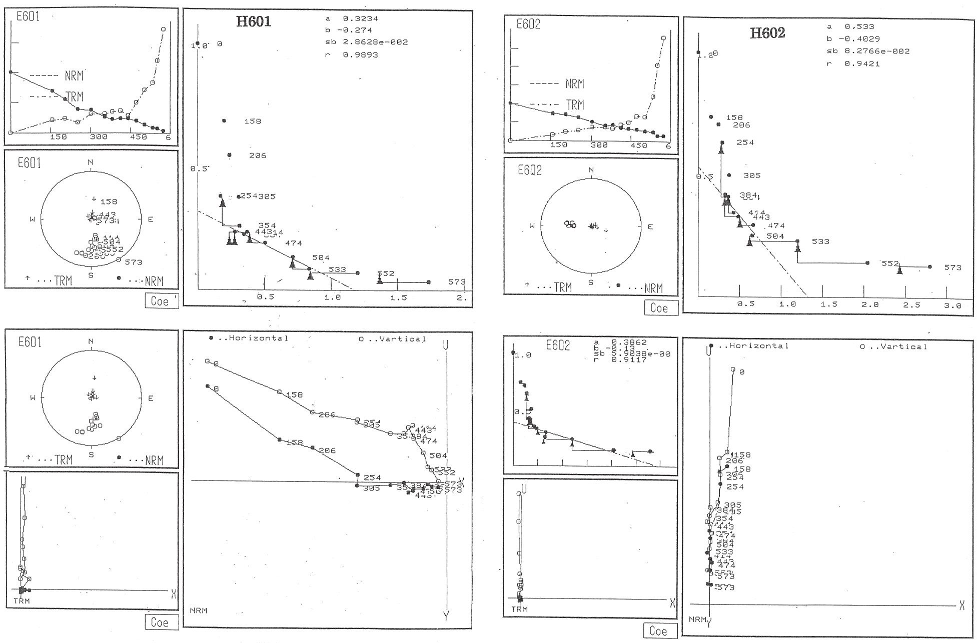

Fig.9-7 Arai Diagram of the Hishikari Lower (N) : H_0=50μT

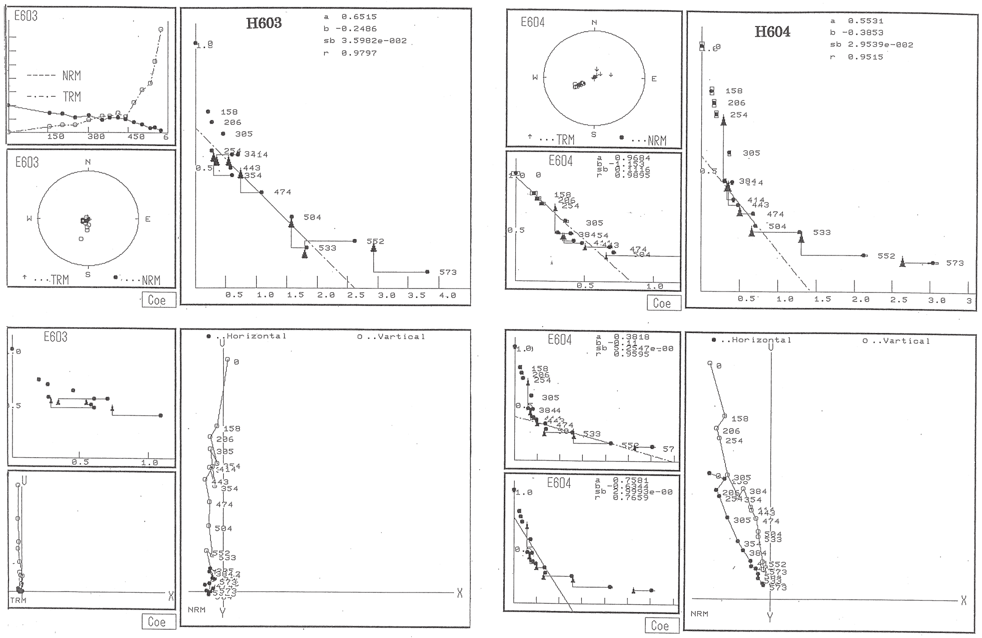

Fig.9-8 Arai Diagram of the Hishikari Lower (N): H_0=50μT

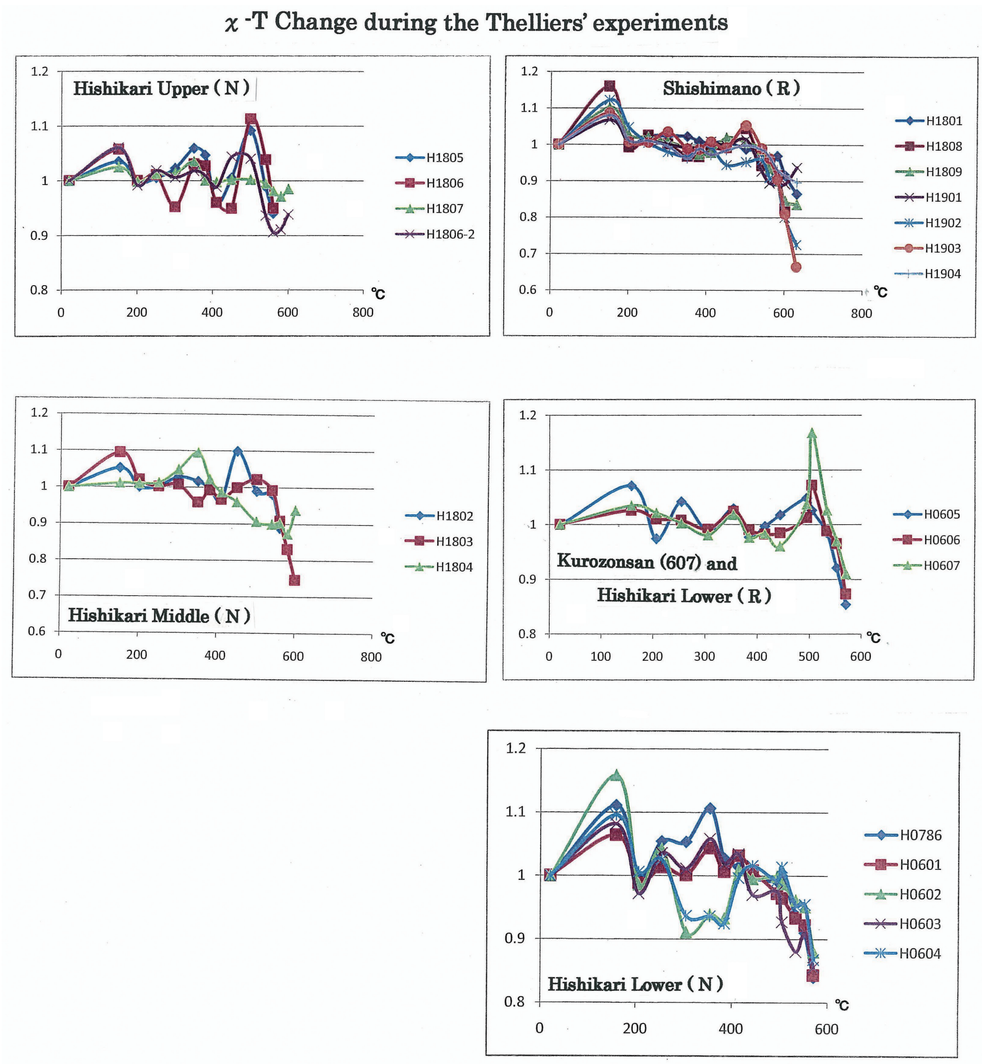

Fig.10 χ-T change during the Thelliers' experiments

1. To find out the maximum temperature, under which no significant thermo-chemical alteration occurs during the experiments.
2. To satisfy pTRM1=pTRM2, under this maximum temperature in the duplicate experiments of TRM addition.
3. Under this maximum temperature, to ascertain that unblocking temperature spectra of NRM and TRM coincide in some temperature range.
4. Paleointensity data calculated from the individual temperature ranges must follow a normal distribution.

To select the suitable samples for Zheng's method, χ-T measurement by KLY-3S

Kappabridge magnetic susceptibility meter was performed on the samples which were selected by the naked eye observation (Fig.11-1~Fig.11-3). The first run started from the room temperature to 450 ℃, after cooling to the room temperature, the second run started up to 550℃, the third run to 650℃. If the repeated lines overlap each other, chemical change and interaction effect had not occurred. In the Fig.11, the minimum change of lines can be seen in sample H1801. Then, this sample was selected for Zheng's method experiment. Some other samples were also used in the experiment for comparison.

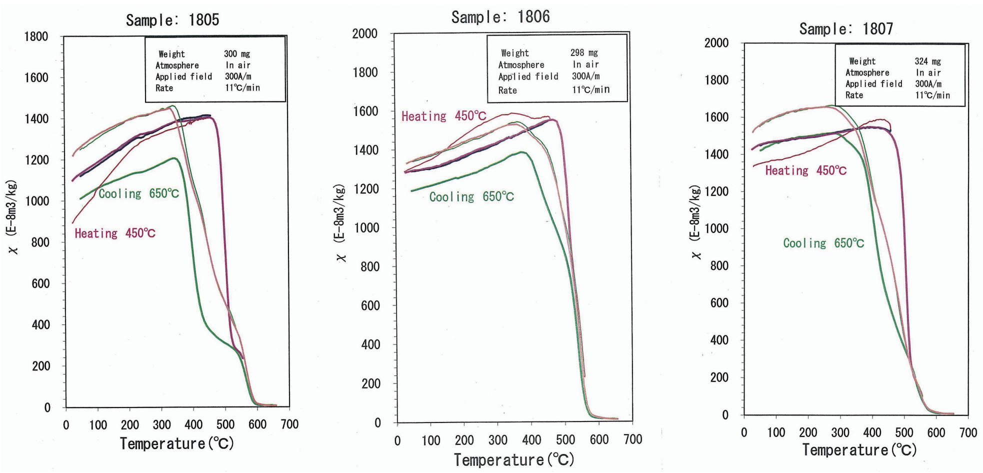

Fig.11-1 χ-T change by Kapper Bridge of Hishikari Upper (N)

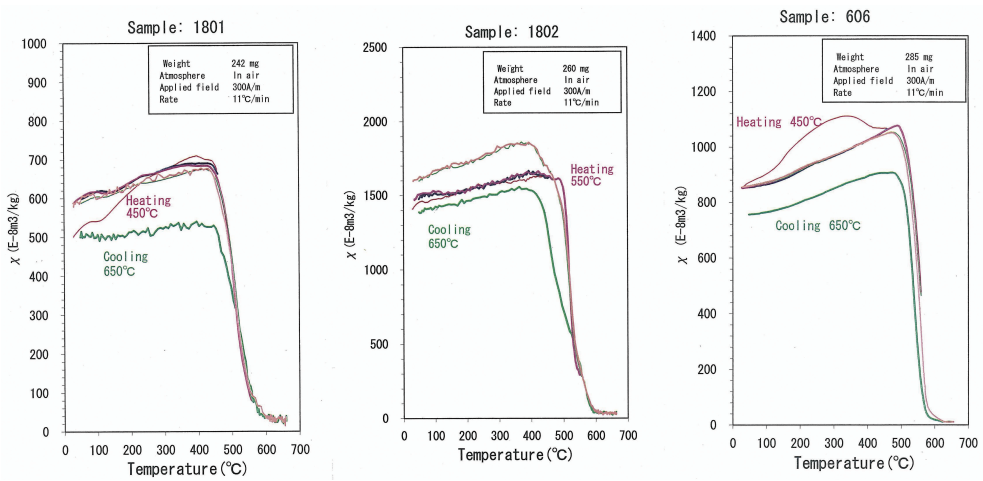

Fig.11-2 χ-T change by Kapper Bridge of H1801 : Shishimano (R), H1802 : Hishikari Middle (N), H606 : Hishikari Lower (R)

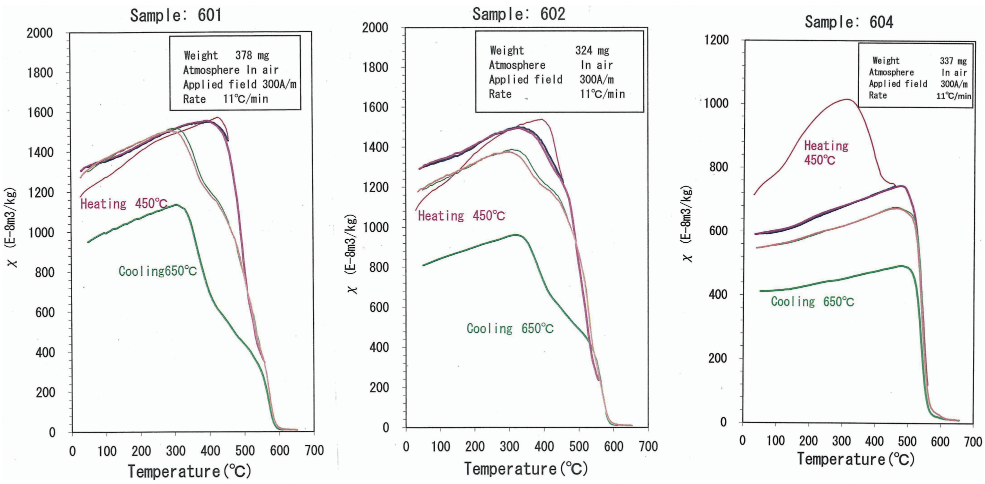

Fig.11-3 χ-T change by Kapper Bridge of Hishikari Lower (N)

5-1 Quick Method

Thermal demagnetization of NRM was carried on five samples (including sample H1801) to yield unblocking temperature spectra. Next, after being heated over 590℃ the sample was cooled to room temperature in the laboratory field of 50μT to acquire a full TRM, thermal demagnetization was carried again to yield unblocking temperature spectra of this full TRM in the same temperature steps as NRM (Fig.12-1~ Fig.12-5). Comparison of those two unblocking spectra of TRM and NRM yields a paleointensity data from each unblocking temperature interval (Table 3).

Except for sample H1801, paleointensity data from individual unblocking temperature intervals of each specimen are widely scattered. Only the specimen H1801 showed good consistent results with average of 46+/−3μT by directly comparison of unblocking spectra of NRM with that of TRM (quick version of Zheng's method). The coincidence of unblocking spectra pattern of NRM and TRM of H1801 suggests that the chemical change might have not occurred during laboratory heating, assuring that the NRM were originated from TRM. On the other side, specimens H1806, H1802, H606 and H604 were suffered from chemical changes during heating, thus resulting the different patterns of unblocking spectra between NRM and TRM.

The chemical alteration of the magnetic minerals estimated by the difference of unblocking spectra pattern of NRM and TRM could be the main reasons of the failure in previous Thelliers' method illustrated in Fig.9-1~ Fig.9-8.

The comparison of unblocking spectra pattern of duplicate thermal demagnetization might indicate the chemical change of the magnetic minerals during experiment. Magneto-static interaction effect is another reason which resulting off-line behavior in Arai diagram. If there

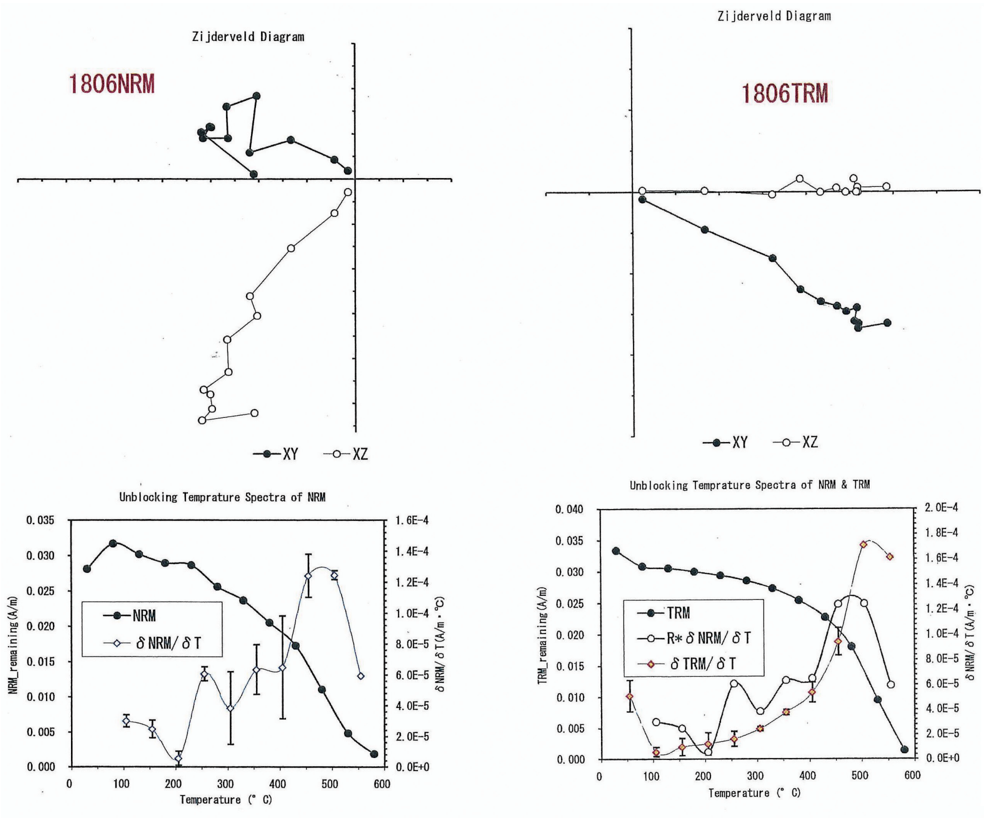

Fig.12-1 Unblocking Temperature Spectra of H1806 :Hishikari Upper (N)

Table 3. H_{an} calculated from Unblocking Temperature Spectra (see Fig.12) in easy method.

Unblocking Temp. ℃	H1806 (Hishikari Upper)	H1801 (Shishimano)	H1802 (Hishikari Middle)	H606 (Kurozonsan)	H604 (Hishikari Lower)
30	8	43	35	8	26
30-80	10	44	32	8	23
80-130	10	44	29	7	20
130-180	10	44	27	7	19
180-230	10	45	26	7	18
230-280	9	44	22	6	13
280-330	9	45	18	5	9
330-380	8	46	15	4	11
380-430	8	48	4	4	7
430-480	6	52	2	3	7
480-530	5	52	-	-	-
530-580	13	44	-	-	-
580-590	-	-	-	-	-
Mean	8	46	25	7	18
Error	2	3	6	1	6

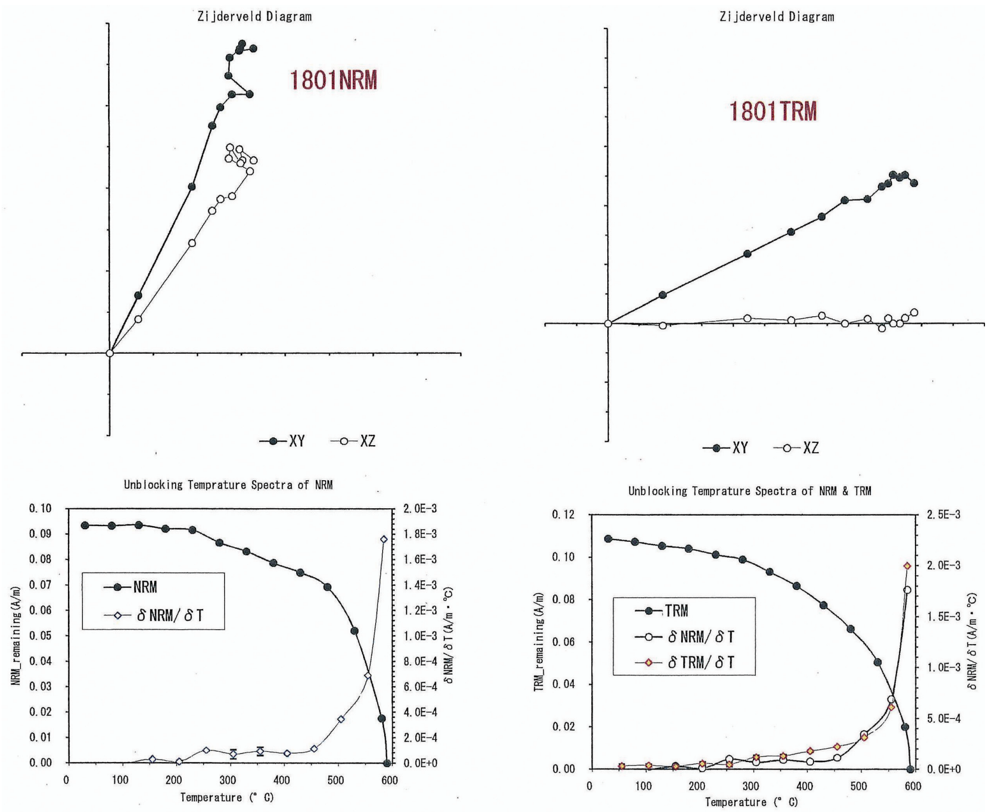

Fig.12-2 Unblocking Temperature Spectra of H1801 : Shishimano (R)

is the large interaction effect, large scattered distribution of H_{an} can be expected, thus resulting off straight-line behavior in Arai diagram. In this case, a H_{an} calculated from Arai diagram (apparent H_{an}) is far from the genuine one. Small interaction effect only makes small dispersive distribution of H_{an}, and makes almost straight line in Arai diagram to obtain a data near its genuine. The difference between the genuine H_{an} and apparent H_{an} depends on the distribution of unblocking temperature of interacting-grains. Large difference in distribution of unblocking temperature of interacting-grains produces a large difference between the genuine H_{an} and apparent H_{an}. Similar unblocking temperature of interacting grains contributes to get the near genuine apparent H_{an}. It must also notice there is existence the case when apparent H_{an} from each individual temperature intervals would be quite different from the genuine one while if it is of a small dispersive distribution would still make faked straight line in Arai diagram.

Coincidence was noticed between χ-T change (Fig.11-1 ~ Fig.11-3) and unblocking spectra pattern of NRM and TRM (Fig.12-1 ~ Fig.12-5). Only sample H1801 (Fig.11-2) shows the good reproducibility in the repeated analysis. On the other hand, reproducibility could not be

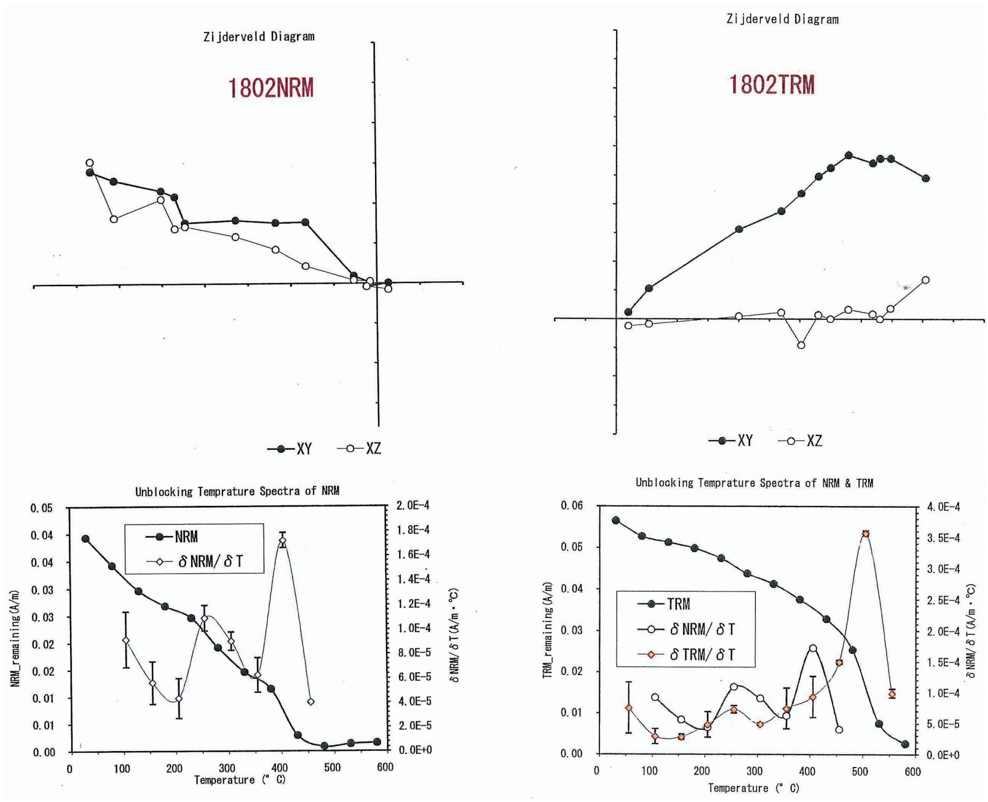

Fig.12-3 Unblocking Temperature Spectra of H1802 : Hishikari Middle (N)

found in other specimens, due to the chemical change during the laboratory heating.

5-2 Zheng's method applied to H1801

Five specimens from the sample H1801 were selected for Zheng's method under the suggestion of pilot in quick measurement.

1^{st} RUN (pick-up run)

In Zheng method, the 1^{st} RUN (pick-up run) is a "differentiated Thellier method".
For every temperature interval (T_{i+1}, T_i), we measure the following two terms:

$$pTRM1(T_{i+1}, T_i, H_{lab}) \text{ and}$$
$$\delta NRM(T_{i+1}, T_i) = NRM(T_i)_{remaining} - NRM(T_{i+1})_{remaining}$$

Then, an apparent paleointsnsity $H_{an\text{-}1}$ can be estimated
(Differentiated Thellier method)

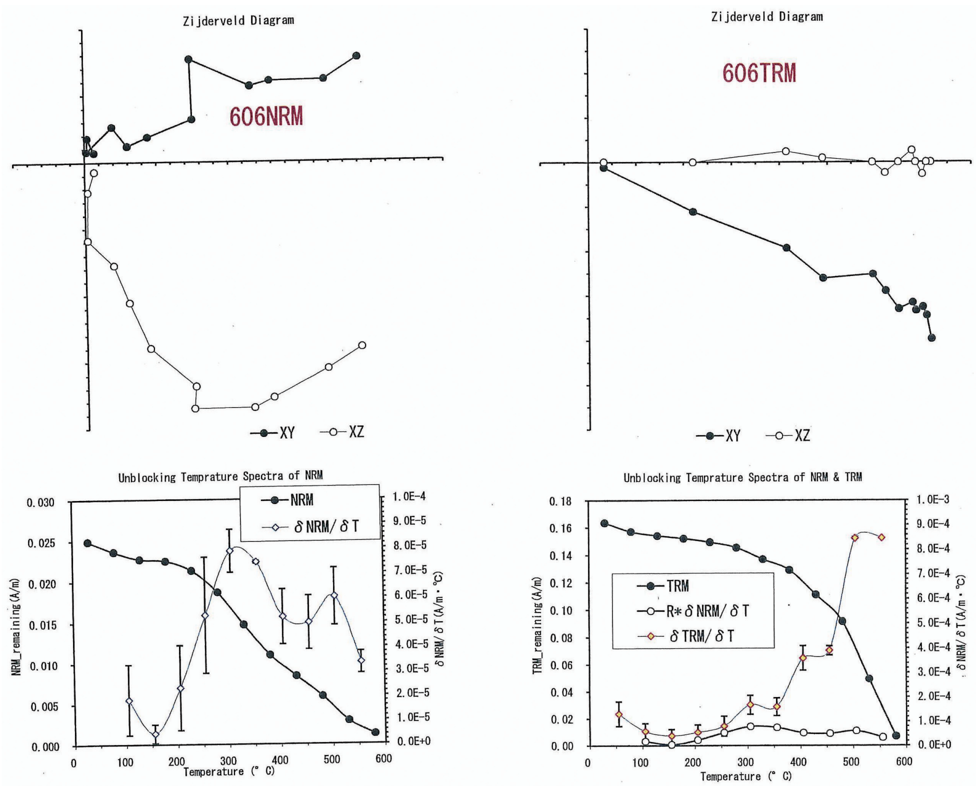

Fig.12-4 Unblocking Temperature Spectra of H606 : Hishikari Lower (R)

$$H_{an\text{-}1} = \delta NRM(T_{i+1},T_i) / pTRM1(T_{i+1},T_i, H_{lab}) * H_{lab} \tag{1}$$

Thermal demagnetization of NRM was conducted step-wisely (T_{i+1}) to obtain an individual δNRM(T_{i+1},T_i). Then at every individual temperature interval (T_{i+1},T_i), pTRM1(T_{i+1},T_i, H_{lab}) was acquired by cooling from temperature T_{i+1} to T_i in a laboratory field of H_{lab} (100μT), a field which was applied in perpendicular direction of NRM, and this field H_{lab} was switched off when cooling from temperature T_i to room temperature. Comparison of the these two δNRM(T_{i+1},T_i) and pTRM1(T_{i+1},T_i, H_{lab}) yielded a apparent paleointensity ($H_{an\text{-}1}$). The detail of the results were shown in Fig.13-1, 13-3, 13-5, 13-7 and 13-9. Arai diagram did not follow a straight line because of the chemical change or affect of magneto-static interaction between the magnetic grains. To correct the interaction effect, the 2nd run was performed.

2nd RUN

In the experiment of 2nd RUN (correction run), the same specimen is used to acquire a $TRM_{lab\text{-}2}$ to correct the interaction affect.

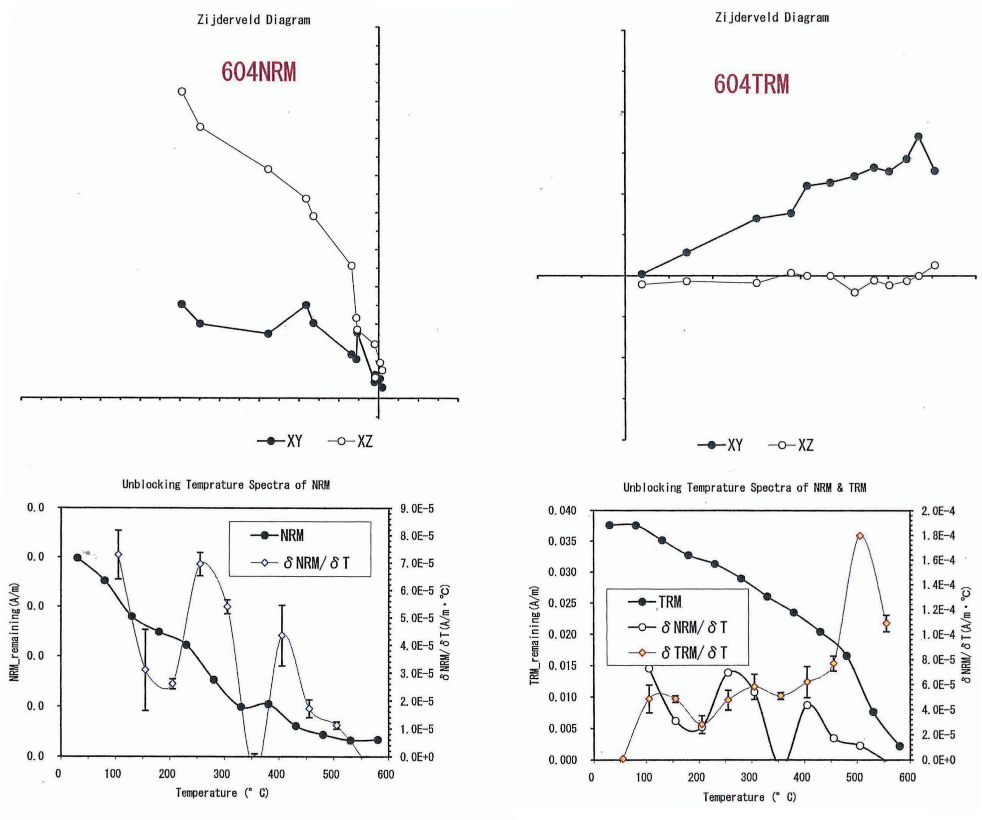

Fig.12-5 Unblocking Temperature Spectra of H604 : Hishikari Lower (N)

TRM_{lab-2} is acquired cooling from thermal alteration safeguard maximum temperature T_n to room temperature in an artificial field H_{lab-2} as close as possible to ancient magnetic field intensity (H_{an}) at a given low cooling rate 1℃/min. And the artificial field is applied to the sample in the same direction of NRM.

In this way, the obtained TRM_{lab-2} is a TRM of property nearest that of full_TRM.

$$TRM_{lab-2} = TRM(T_n, T_0, H_{lab\_2}) + NRM(T_n)_{\_remaining} \quad (2)$$

In the second run, TRM_{lab-2} is used instead of NRM, the same process as 1st RUN, to get $pTRM2(T_{i+1},T_i)$ and $\delta TRM_{\_lab-2}(T_{i+1},T_i)$ and H_{an-2}

$$H_{an-2} = \delta TRM_{\_lab-2}\ (T_{i+1},T_i)\ /pTRM2(T_{i+1},T_i,H_{lab})\ *\ H_{lab} \quad (3)$$

(Continued on page 172)

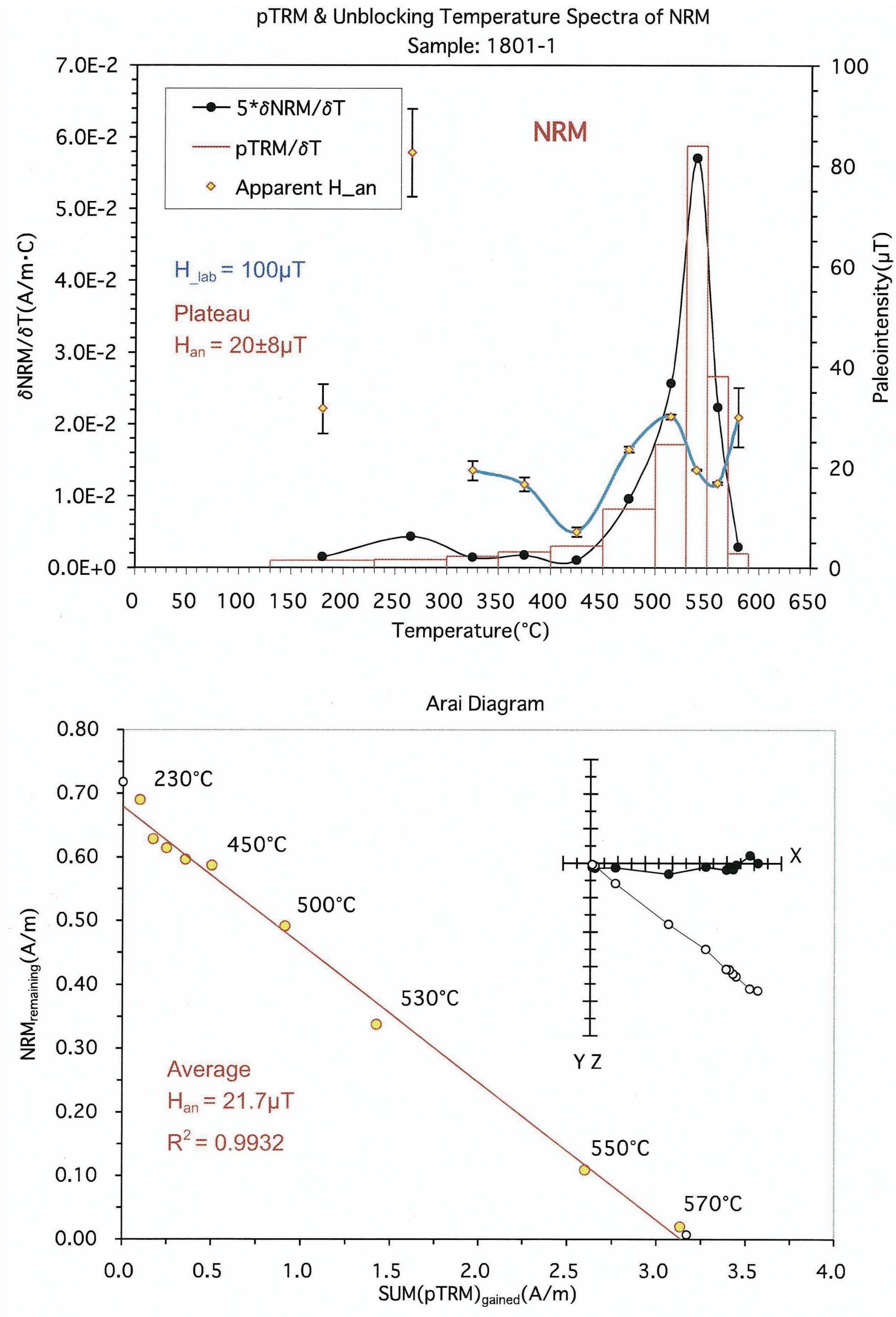

Fig.13-1 1st RUN (Pick up) — pTRM & Unblocking Temperature Spectra of NRM on H1801-1

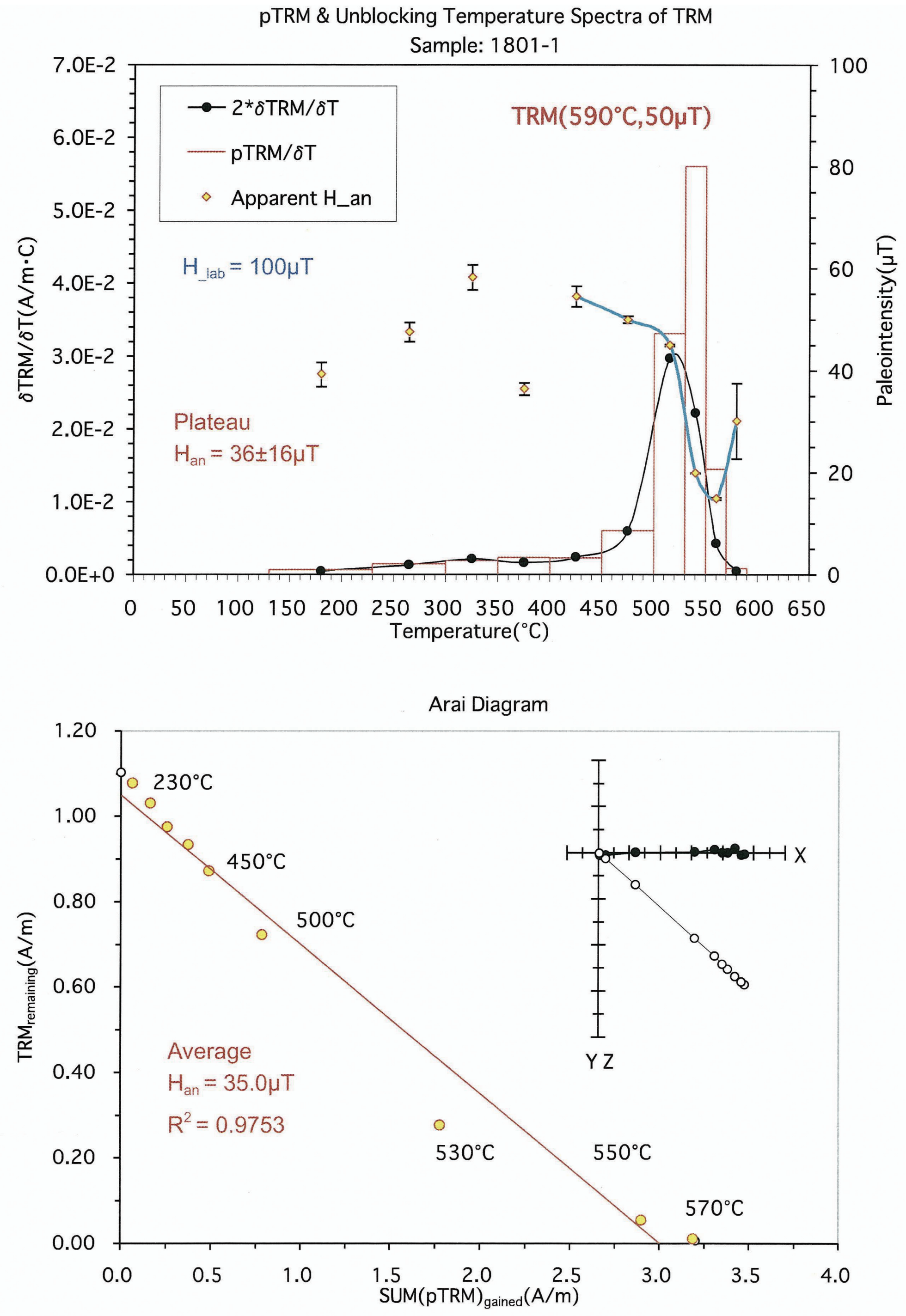

Fig.13-2 2nd RUN (Correction) — pTRM & Unblocking Temperature Spectra of TRM on H1801-1

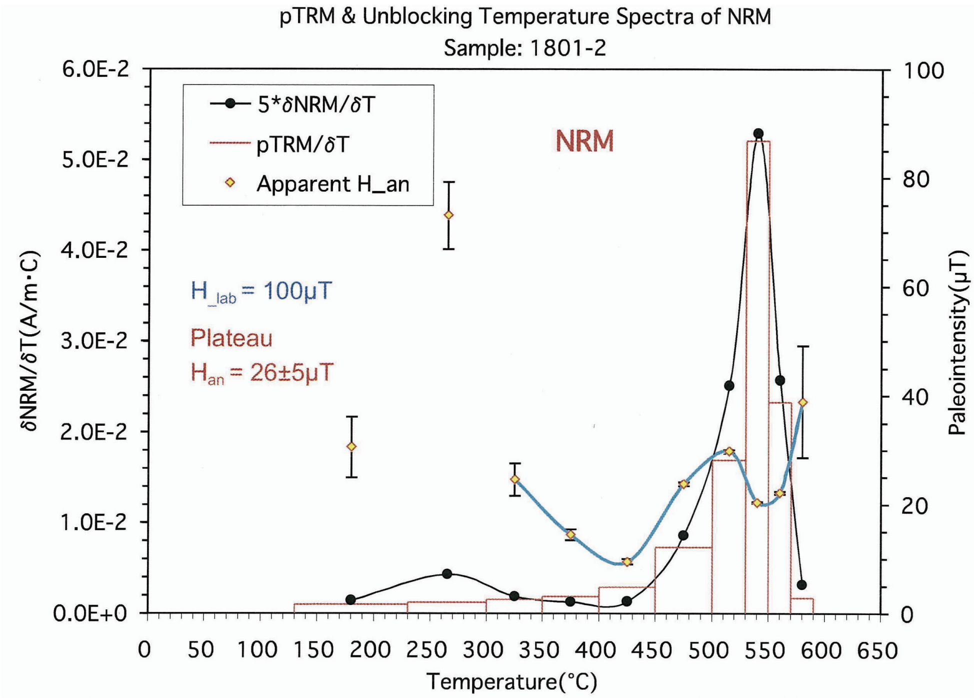

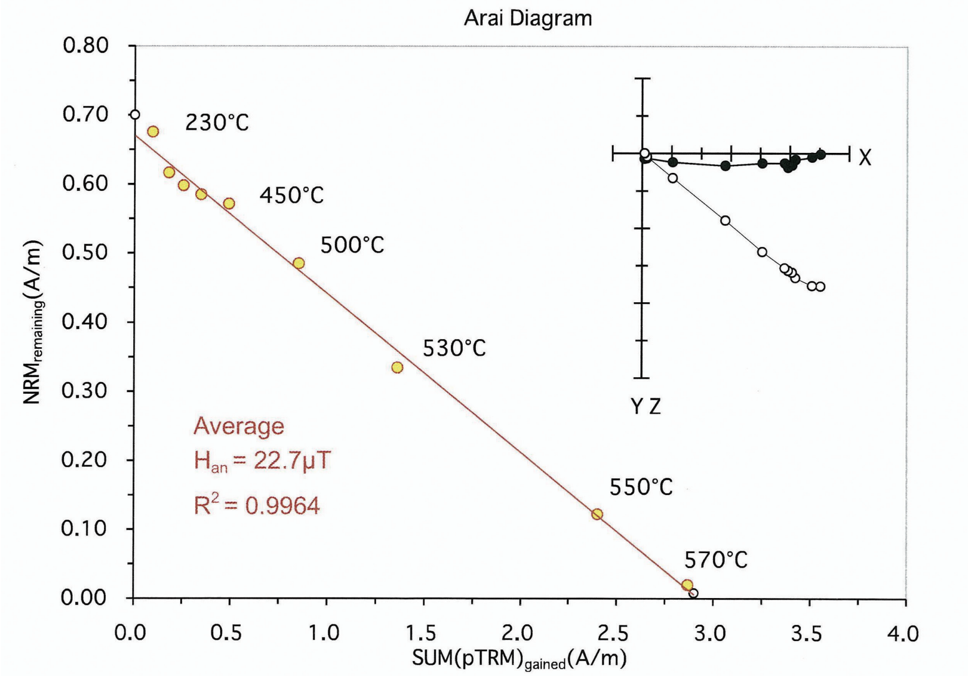

Fig.13-3 1st RUN (Pick up) — pTRM & Unblocking Temperature Spectra of NRM on H1801-2

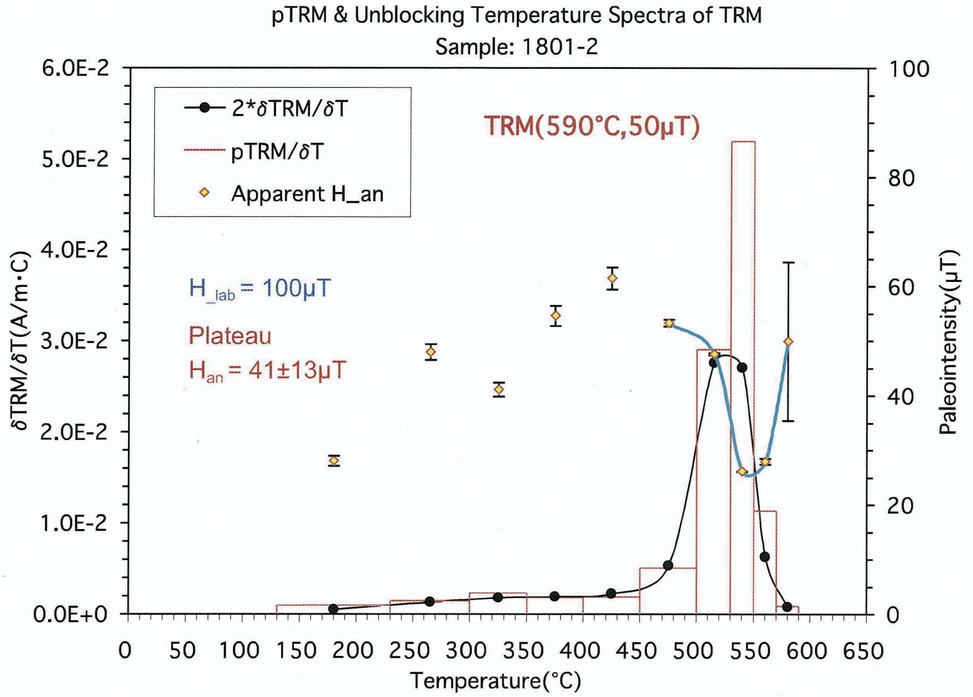

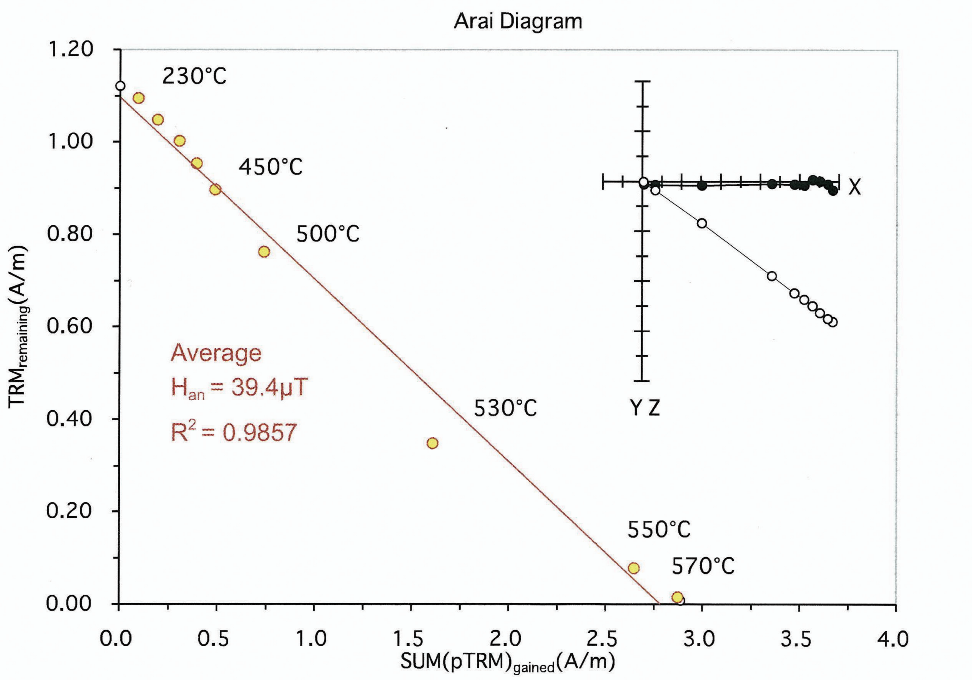

Fig.13-4 2nd RUN (Correction) — pTRM & Unblocking Temperature Spectra of TRM on H1801-2

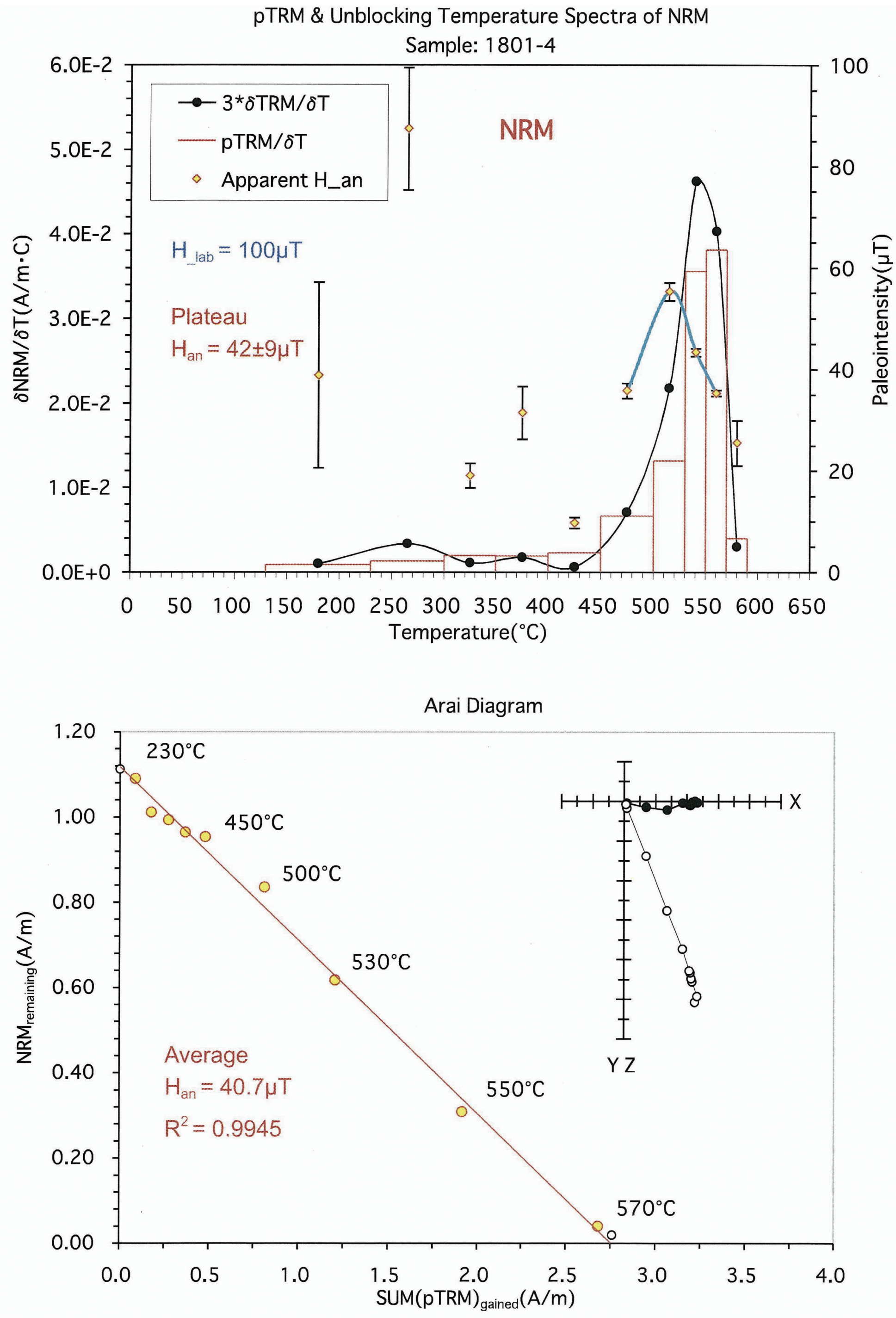

Fig.13-5 1[st] RUN (Pick up) — pTRM & Unblocking Temperature Spectra of NRM on H1801-4

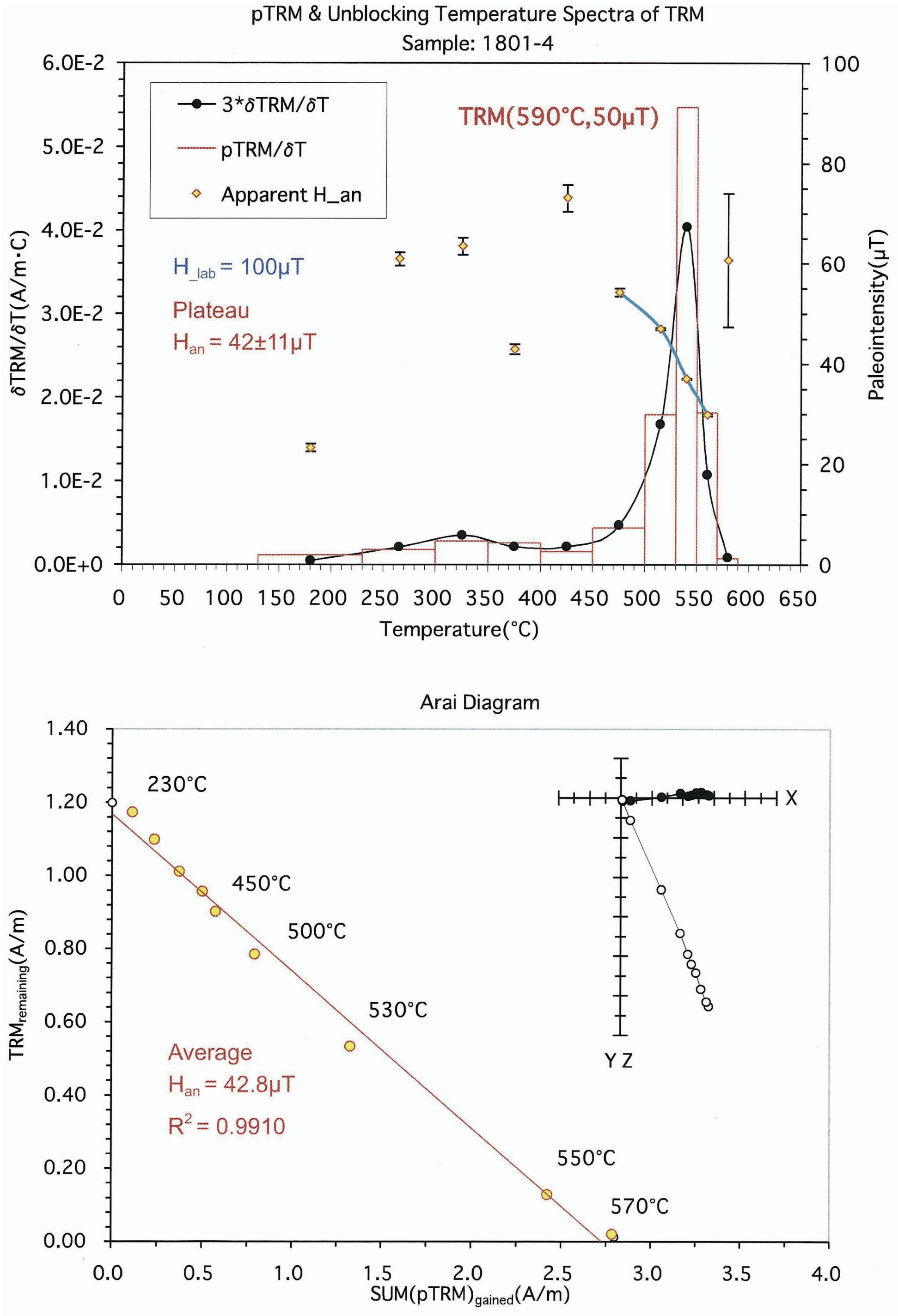

Fig.13-6 2nd RUN (Correction) — pTRM & Unblocking Temperature Spectra of TRM on H1801-4

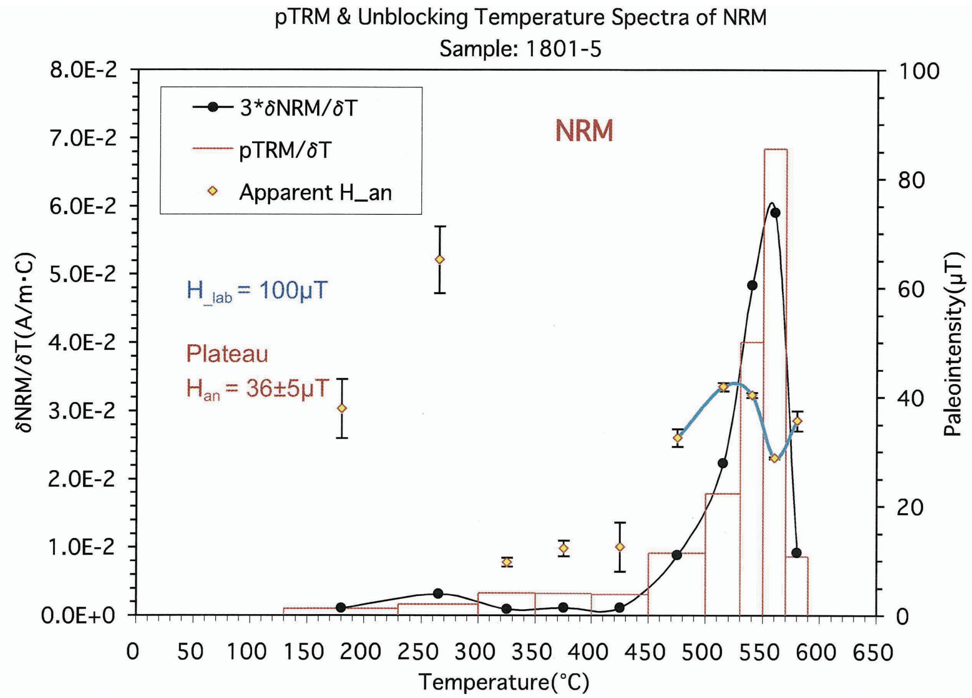

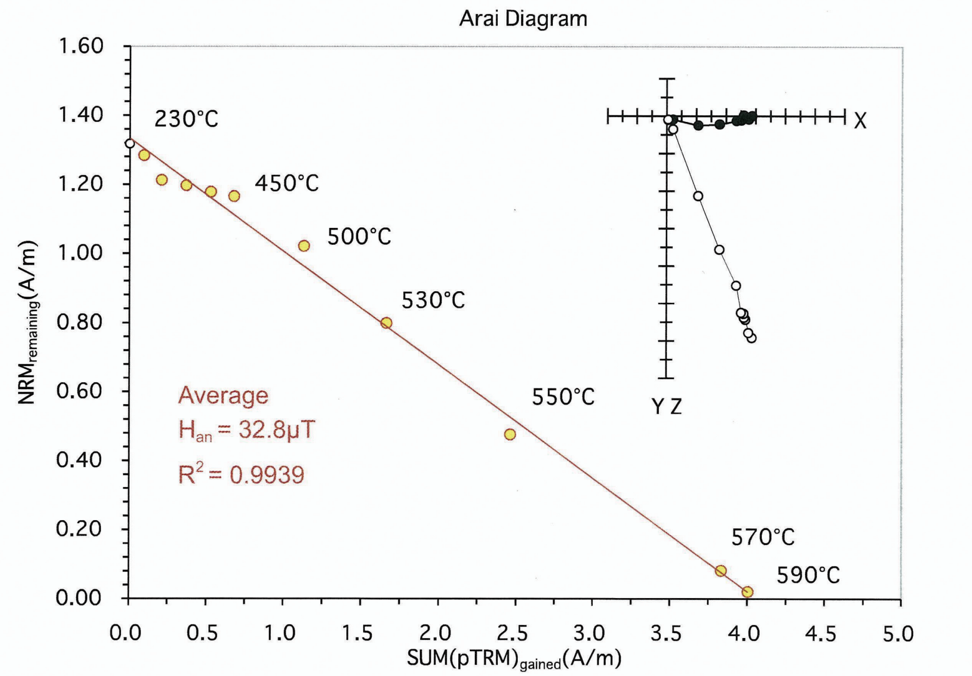

Fig.13-7 1st RUN (Pick up) — pTRM & Unblocking Temperature Spectra of NRM on H1801-5

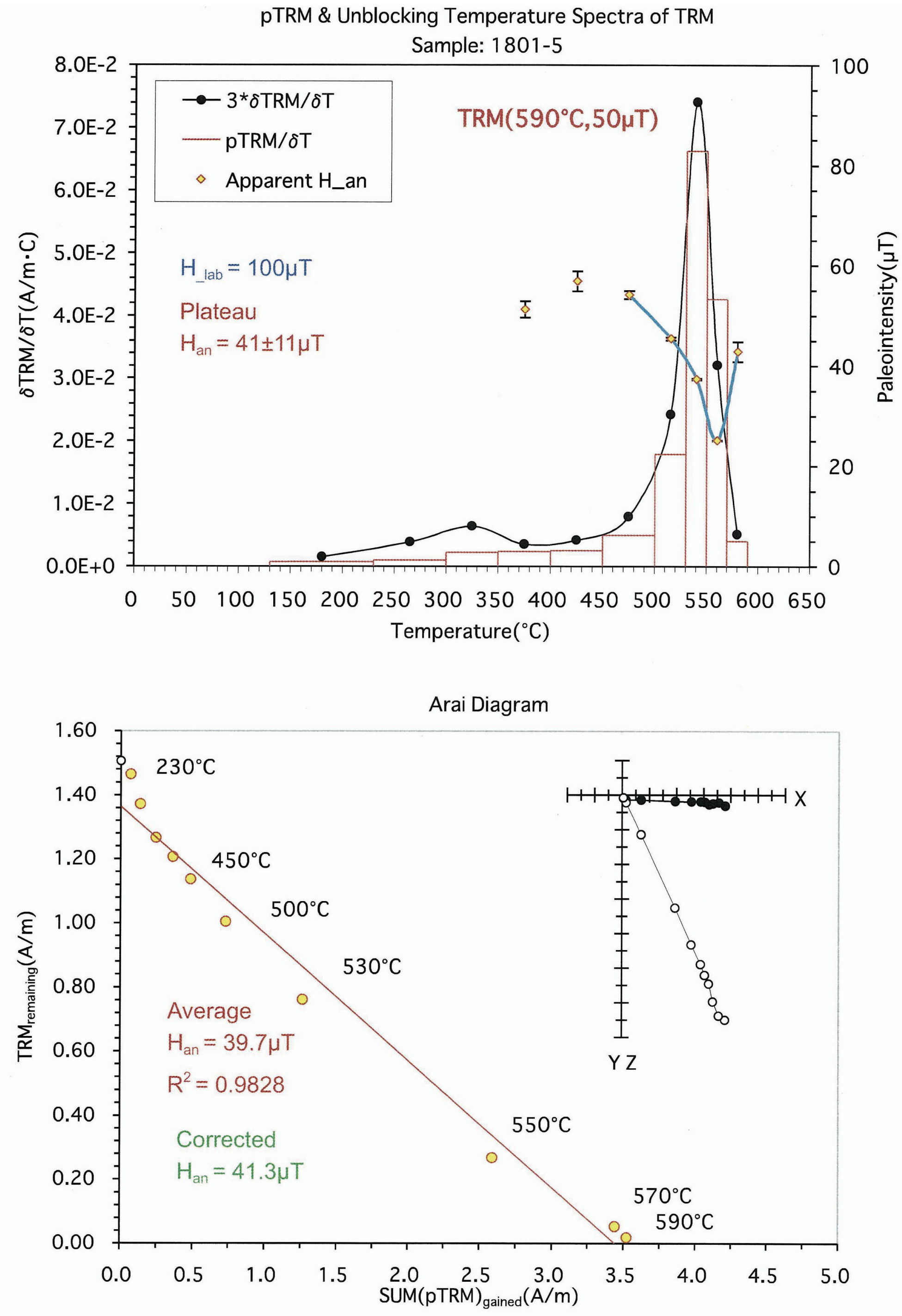

Fig.13-8 2[nd] RUN (Correction) — pTRM & Unblocking Temperature Spectra of TRM on H1801-5

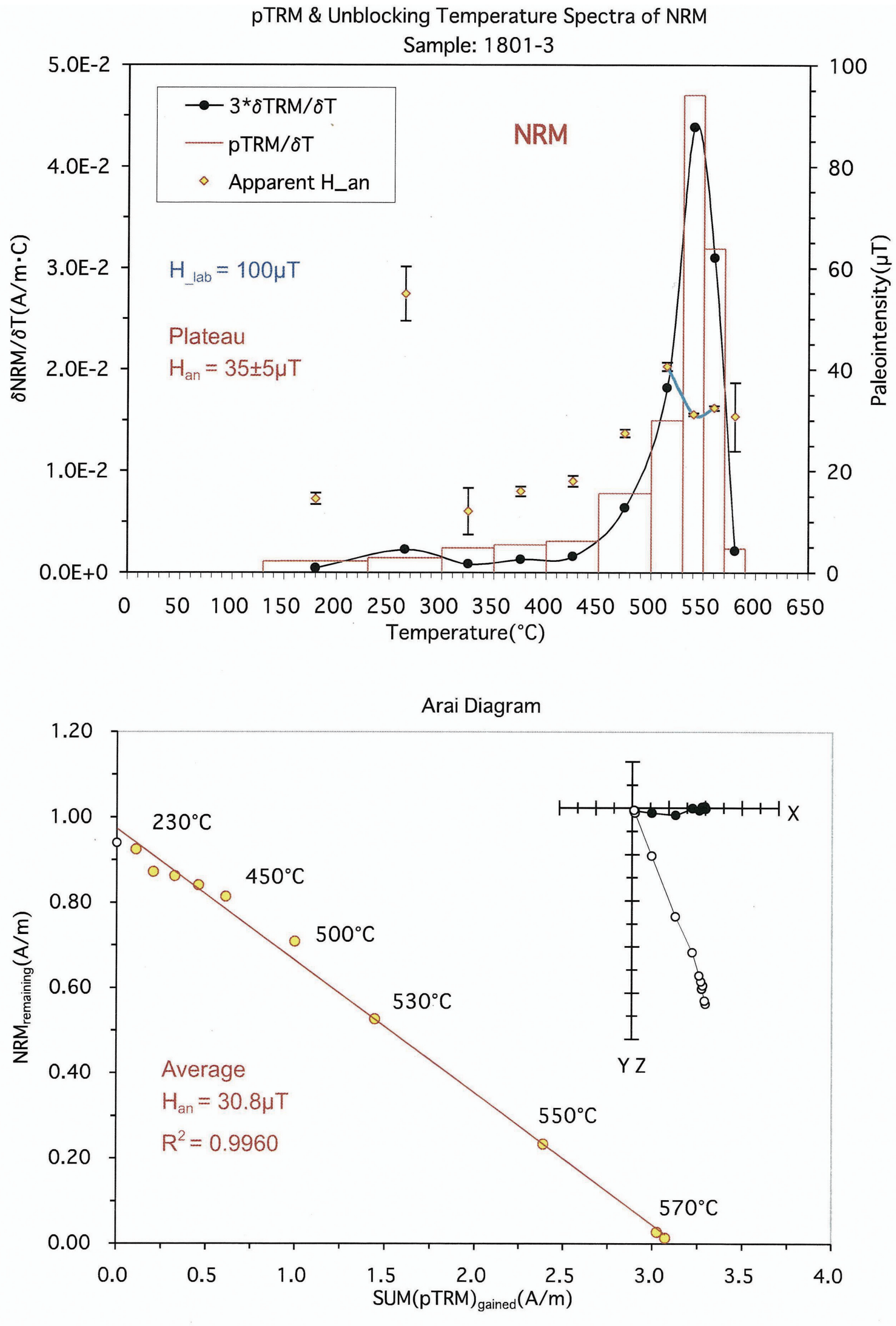

Fig.13-9 1st RUN (Pick up) — pTRM & Unblocking Temperature Spectra of NRM on H1801-3

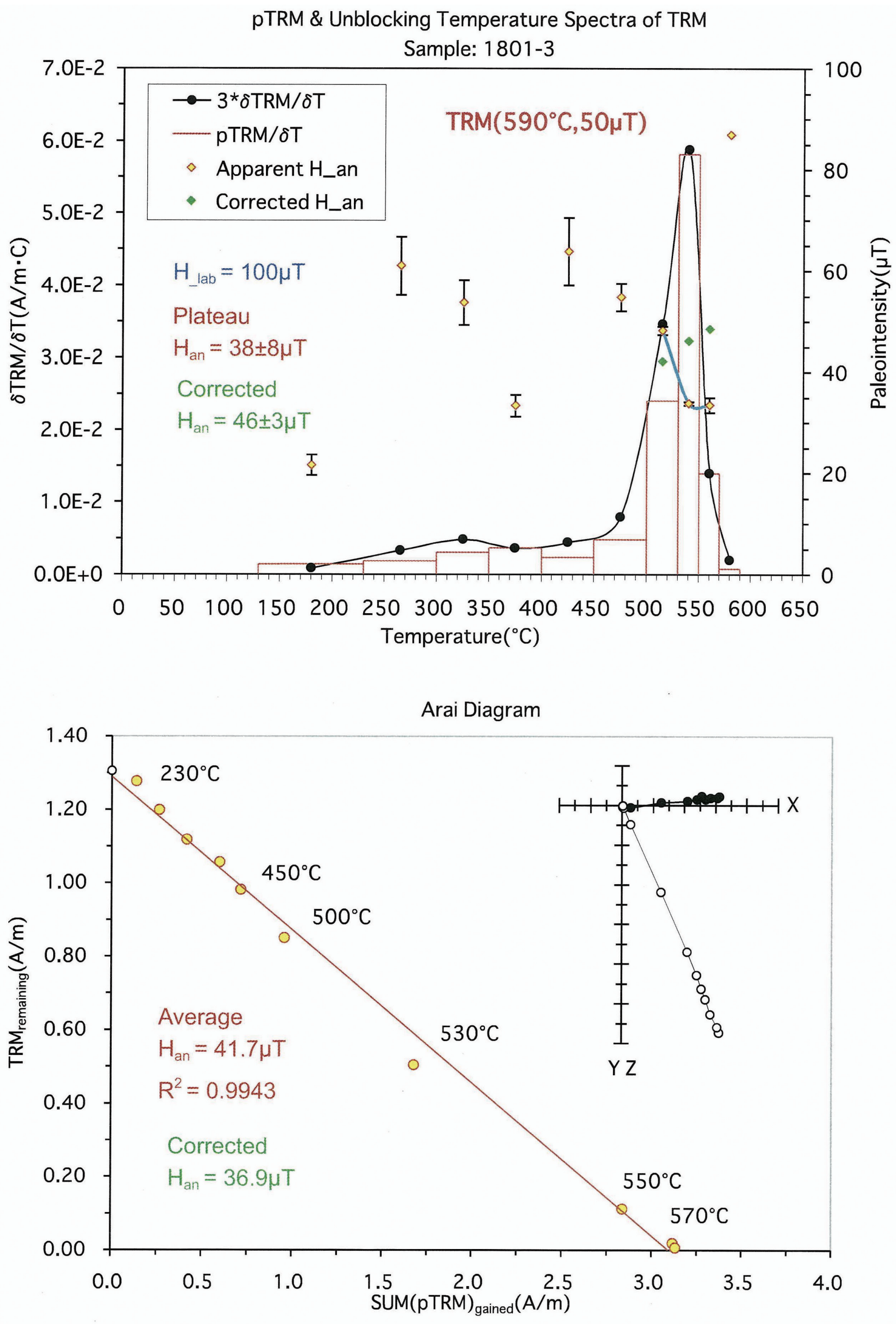

Fig.13-10 2nd RUN (Correction) — pTRM & Unblocking Temperature Spectra of TRM on H1801-3

If no significant thermal alteration occurs during the experiment, pTRM2(T_{i+1},T_i) will be almost equal to pTRM1(T_{i+1},T_i). The proportional part of δTRM$_{_lab\text{-}2}$(T_{i+1},T_i) and δNRM(T_{i+1},T_i) will be used to estimate genuine paleointensity (Corrected H_{an}).

$$\text{Corrected } H_{an} = (H_{lab\text{-}1} / H_{an\text{-}2}) * H_{an\_1} \quad (4)$$

In the 2nd run of this time, we selected T_n to be 590 ℃ and a laboratory field to be 50μT, thus a full TRM was acquired.

The results of second run are illustrated in Fig.13-2, 13-4, 13-6, 13-8 and 13-10. Similarly to the 1st run, Arai diagram did not make the straight line because of the interaction effect.

Only specimen H1801-3 (Fig.13-10) meets the condition for interaction correction: blocking temperature spectra pTRM2(T_{i+1},T_i) are almost equal to pTRM1(T_{i+1},T_i), and do exists proportional part of δTRM$_{_lab\text{-}2}$(T_{i+1},T_i) and δNRM(T_{i+1},T_i). Three temperature intervals, 500 ℃~530 ℃, 530 ℃~550 ℃ and 550 ℃~570 ℃ were used to obtained a corrected H_{an} with average 46+/−3μT, which is well consistent with that of quick method.

For other four specimens, comparison with first blocking temperature pTRM1(T_{i+1},T_i) the second one pTRM2(T_{i+1},T_i) have shifted toward the low temperature side. Because of thermal alteration, correction of interaction effect could not be performed.

Following shows the detail of correction for specimen H1801-3 (Fig.13-9~Fig.13-10), three temperature intervals were used to obtain a corrected H_{an},

Interval Ⅰ (500℃~530℃), $H_{an\text{-}1}$=41μT, $H_{an\text{-}2}$=48μT
Interval Ⅱ (530℃~550℃), $H_{an\text{-}1}$=31μT, $H_{an\text{-}2}$=34μT
Interval Ⅲ (550℃~570℃), $H_{an\text{-}1}$=32μT, $H_{an\text{-}2}$=33μT

Corrected H_{an} from Interval Ⅰ = (41/48)*50=42.7 μT
Corrected H_{an} from Interval Ⅱ = (31/34)*50=45.6 μT
Corrected H_{an} from Interval Ⅲ = (32/33)*50=48.5 μT
Averaged corrected H_{an}=46+/−3 μT

In the case of the Arai diagram,

Corrected H_{an} = (50/$H_{an\text{-}2}$)* $H_{an\text{-}1}$$\mu$T
= (50/ 41.7)*30.8=36.9μT

6. Result and Conclusion

Pleistcene igneous rocks collected from the Hishikari mining districts were used to extract the paleomagnetic intensities of geomagnetic field. Before the intensity experiments, some experiments to uncover the rockmagnetic properties were also carried out. Hysteresis curve, Curie temperature, hysteresis parameters to make Day diagram were measured by VSM. All of the samples are plotted in pseudo-single domain region in the Day diagram. Duplicate analysis of susceptibility with ascending and descending temperature, reveal the thermo-chemical alteration and unstable remanent magnetic property of rocks during the laboratory heating process. From comparison of unblocking temperature spectra yielded from thermo-demagnetisation of NRM and TRM, the thermo-chemical alteration during the laboratory heating process can also be observed.

Thelliers' method had not derived any straight linear lines in Arai diagram. Zheng's method succeeded only in one sample. The main reasons of the failure to get paleointensity data were thermo-chemical alteration and unstable remanent magnetic property of rocks during the laboratory heating process. For most of the samples, the blocking temperature spectra had shifted toward the lower temperature side after heating. Another failure for Thelliers' method was the effect of magneto-static interaction between grains, which conducted an off-line behavior in Arai diagram, which could not be correctted by Thelliers' method. An exceptional good result from Shishimano dacite by Zheng's method yielded 46+/−3μT, which had been conducted successfully the interaction correction.

As the results, we could not get the paleomagnetic intensity change during the Pleistcene in which 5 times of polar change are well known, from igneous rocks collected from the Hishikari mining districts. However we could get excellent information and data for the future paleomagnetic study.

References

Metal Mining Agency of Japan and Sumitomo Metal Mining Co.,Ltd. (1987), Discovery and development of Hishikari mine. Mining Geology, 37 (4), 227-236 (in Japanese with English abstract).

Ueno, H., M. Nedachi, Y. Urashima, K. Ibaragi and R. Suzuki (1987), Paleomagnetism of the Hishikari Gold Deposits; Preliminary Report. Rock Magnetizm and Paleogeophysics, 14, 31-35.

Ueno, H. (2007), Application of the geomagnetic polarity sequence to dating mineral deposits. Andrew et al. (eds) Dgging Deeper: Mineral Explaration and Research, 353-356, Irish Association Economic Geology, Dublin.

Ueno, N., Z. Zheng and T. Sato (2005), Rock magnetic properties of an An-ei Lava, in Sakurajima Volcano – Application to experimental study of geomagnetic paleointensity -. Journal of Toyo Univ.,Natural Science, 49: 111-121.

Ueno, N., Z. Zheng, K. Nemoto and T. Hatta (2008), Thermal analysis of initial susceptibility, isothermal remanence magnetization, surface analysys by X-ray photoelectron spectroscopy and paleointensity determination by the new method, on Unsen Volcanic rocks. Journal of Toyo Univ.,Natural Science, 52: 117-148.

Ueno, N., Z. Zheng (2010), A case study of Unzen Volcanic rocks by using Zheng's method for paleointensity determination. Journal of Toyo Univ.,Natural Science, 54: 107-145.

Ueno, N., Z. Zheng (2011), Paleointensity determination and rock magnetic characters of Miyakejima 1983 lava, Japan. Journal of Toyo Univ.,Natural Science, 55: 163-181

Ueno, N., Z. Zheng (2012), Paleointensity determination of Miyakejima 1983 lava (2). Journal of Toyo Univ.,Natural Science, 56: 177-215.

Z. Zheng, X. Zhao and N. Ueno (2005),Probing and correcting the non-ideal behavior of magnetic grains during Thellier paleointensity experiment: A new method of paleointensity determination (in Japanese with English abstract).Journal of Geograpy, 114(2):258-272.

Z. Zheng, X. Zhao (2006), A new approach for absolute paleointensity determination: Consideration on blocking processes between temperature and interaction field. EOS Trans.AGU,87 (52),Fall Meet. Suppl. Abstract GP21A-1290

Z. Zheng, X. Zhao and C.S. Horng (2010), A new high-precision furnace for paleomagnetic and paleointensity studies: Minimizing magnetic noise generated by heater currents inside traditional thermal demagnetizers. Geochemistry Geophysics Geosystems, 11,Q04Y08,doi :10.1029/2010GC003100.

要旨

菱刈鉱山地域火山岩の古地球磁場強度と磁気特性

上野直子・鄭　重・上野宏共

菱刈鉱山地域には K-Ar 法とフィッショントラック法により、連続的に 0.5my ～ 1.8my に年代測定された第四紀更新世の安山岩（Andesite）と石英安山岩（Dacite）の溶岩が分布している。古地磁気学の研究結果では、それらは BRUNHES と MATUYAMA クロンの境界（0.72Ma）を挟んで、ノーマル(N)とリバース(R)に分かれ、さらに MATUYAMA クロン内で JARAMILLO（0.91~0.97Ma）と OLUDUVAI（1.65~1.88Ma）の 2 つのサブクロン(N)を含んでいる。

当研究の当初の目的は N と R の境界での地球磁場強度の変化を測定することであった。岩石磁気特性は VSM でヒステリシス曲線、ヒステリシスパラメーター、キュリー点を測定した。Day ダイアグラム上では全ての試料が擬似単磁区となった。初期帯磁率を温度を繰り返し昇降しながら測定して、実験中の加熱による化学変化の有無を予想した。また、同じ目的で NRM と TRM を熱消磁して Unblocking Temperature Spectra を作成した。

古地球磁場強度は測定法のうち最もよく使われる古典的なテリエ法及び最近筆者等が開発した鄭法で測定した。テリエ法ではアライダイアグラムで良好な直線が得られなかった。鄭法では 1 試料について 46+/−3μT の信頼できる結果が得られた。

成功率が良くない原因は加熱中に化学変化により磁化強度の温度スペクトルが高温側か

ら低温側に移動するために、粒子間相互作用が完全な補正ができないことである。最も化学変化が少ない獅子間野 Dacite（0.81Ma）の 1 試料（No.1801-3）から鄭法で求められた 46+/−3μT がこの研究で得られた唯一の信頼できる古地球磁場強度である。テリエ法では粒子間相互作用を補正することは出来ない。また、この試料からは、初期段階の実験による NRM と TRM の Unblocking Temperature Spectra の比較からも同じ強度 46+/−3μT が得られている。

採取試料のヒステリシス、Day plot、Js-T、など VSM の磁気特性データは全採取試料間で似通っていた。そのため、VSM データを用いて No.1801 試料を最良の試料として選別することは困難であった。NRM と TRM を熱消磁して Unblocking Temperature Spectra を比較する、あるいは、χ-T　Spectra を繰り返し測定することで選別が可能であった。

結論として、当研究の当初の目的である N と R の境界での地球磁場強度の変化を測定することについては、現在の技法では菱刈鉱山地域の火山岩から強度変化を求めることはできなかった。しかし、今後の古地球磁場強度研究に役立つ多くの岩石磁気的データが得られた。